Oxidative Regulation of Large Conductance Calcium-activated Potassium Channels

Xiang D. Tang,* Heather Daggett,* Markus Hanner,‡ Maria L. Garcia,‡ Owen B. McManus,‡ Nathan Brot,§ Herbert Weissbach,‖ Stefan H. Heinemann,¶ and Toshinori Hoshi*

From the *Department of Physiology and Biophysics, The University of Iowa, Iowa City, Iowa 52242; ‡Merck Research Laboratories, Rahway, New Jersey 07065; §Hospital for Special Surgery, Cornell University Medical Center, New York, New York 10021; ‖Center for Molecular Biology and Biotechnology, Florida Atlantic University, Boca Raton, Florida 33431; and ¶AG Molekulare und Zelluläre Biophysik am Klinikum der Universitat Jena, D-07447 Jena, Germany.

ABSTRACT Reactive oxygen/nitrogen species are readily generated in vivo, playing roles in many physiological and pathological conditions, such as Alzheimer's disease and Parkinson's disease, by oxidatively modifying various proteins. Previous studies indicate that large conductance Ca^{2+}-activated K^+ channels (BK_{Ca} or Slo) are subject to redox regulation. However, conflicting results exist whether oxidation increases or decreases the channel activity. We used chloramine-T, which preferentially oxidizes methionine, to examine the functional consequences of methionine oxidation in the cloned human Slo (*h*Slo) channel expressed in mammalian cells. In the virtual absence of Ca^{2+}, the oxidant shifted the steady-state macroscopic conductance to a more negative direction and slowed deactivation. The results obtained suggest that oxidation enhances specific voltage-dependent opening transitions and slows the rate-limiting closing transition. Enhancement of the *h*Slo activity was partially reversed by the enzyme peptide methionine sulfoxide reductase, suggesting that the upregulation is mediated by methionine oxidation. In contrast, hydrogen peroxide and cysteine-specific reagents, DTNB, MTSEA, and PCMB, decreased the channel activity. Chloramine-T was much less effective when concurrently applied with the K^+ channel blocker TEA, which is consistent with the possibility that the target methionine lies within the channel pore. Regulation of the Slo channel by methionine oxidation may represent an important link between cellular electrical excitability and metabolism.

KEY WORDS: chloramine-T • methionine • methionine sulfoxide • methionine sulfoxide reductase • cysteine

INTRODUCTION

Large conductance Ca^{2+}-activated K^+ channels (BK_{Ca} or Slo)[1] are ubiquitously present and play a variety of physiological roles, generally providing an inhibitory negative feedback influence that links cellular metabolism and excitability (Marty, 1989; McManus, 1991; Toro and Stefani, 1991; Jan and Jan, 1997; Toro et al., 1998; Vergara et al., 1998). The physiological importance of BK_{Ca} channels has been well documented in regulation of the vascular tone (Brayden, 1996; Rusch et al., 1996; Brenner et al., 2000; Pluger et al., 2000), neurosecretion (Lingle et al., 1996), and cochlear frequency tuning (Fettiplace and Fuchs, 1999; Ramanathan et al., 1999).

BK_{Ca} or Slo channels are characterized by their large single-channel openings (>200 pS in symmetrical 100 mM KCl) and voltage-dependent activation modulated by intracellular Ca^{2+} (Latorre et al., 1984; Pallotta et al., 1992; Kaczorowski et al., 1996; Meera et al., 1996; Cui et al., 1997; Jan and Jan, 1997; Atkinson et al., 1998; Vergara et al., 1998; Horrigan et al., 1999). Although its activation is favored by Ca^{2+}, the Slo channel may be fully activated by depolarization alone without Ca^{2+} (Cui et al., 1997). The amino acid sequences of the Slo α subunits, originally isolated from *Drosophila* (Atkinson et al., 1991; Adelman et al., 1992), indicate that each subunit has a "core" domain and the COOH "tail" domain. The structural organization of the core domain is similar to that of *Shaker*-type voltage-gated Kv channels, in that it contains six putative transmembrane segments (S1–S6) and the pore (P) segment. The S4 segment contains several positively charged amino acid residues that are involved in voltage-dependent gating of the Slo channel (Noceti et al., 1996; Stefani et al., 1997; Diaz et al., 1998). The Slo core domain also includes the S0 segment in the NH_2 terminus, such that the NH_2-terminal end faces the

The current address for M. Hanner is INTERCELL, Rennweg 95B, A-1030 Wien, Austria.

Address correspondence to Toshinori Hoshi, Department of Physiology and Biophysics, The University of Iowa, BSB 5-660, Iowa City, IA 52242. Fax: (319) 353-5541; E-mail: hoshi@hoshi.org

[1]*Abbreviations used in this paper:* BK_{Ca} channels, large conductance calcium-activated potassium channels; Ch-T, chloramine-T; DTNB, 5,5′-dithio-bis(2-nitrobenzoic acid); DTT, dithiothreitol; met(O), methionine sulfoxide; MSRA, peptide methionine sulfoxide reductase; MTSEA, methanethiosulfonate ethylammonium; NO, nitric oxide; PCMB, p-chloromercuribenzoic acid; Q_{app}, apparent equivalent charge movement; ROS/RNS, reactive oxygen/nitrogen species; $V_{0.5}$, half-activation voltage.

extracellular side (Meera et al., 1997). This domain at least, in part, mediates the interaction of Slo with the auxiliary β subunit (Wallner et al., 1996), which increases the overall activity of the channel largely in a Ca^{2+}-independent manner (Nimigean and Magleby, 2000). The long tail domain of the Slo subunit is considered to be cytoplasmic (Meera et al., 1997) and contributes to the Ca^{2+} sensitivity of the channel (Wei et al., 1994; Schreiber and Salkoff, 1997), possibly by forming a Ca^{2+} binding motif termed the calcium bowl (Schreiber and Salkoff, 1997). Within the tail domain, multiple subdomains may be involved in mediating the Ca^{2+} sensitivity (Schreiber et al., 1999). As found with voltage-gated Kv channels, it is likely that four Slo subunits form one functional channel (Shen et al., 1994) with or without β subunits depending on the cell type (Chang et al., 1997; Tanaka et al., 1997; Wanner et al., 1999).

Gating of BK_{Ca} channels has been extensively studied both in native and heterologous expression systems. Single-channel studies show that the Slo or BK_{Ca} channel displays bursts of openings with short flicker closures involving multiple dwell time components (Barrett et al., 1982; Methfessel and Boheim, 1982; Moczydlowski and Latorre, 1983; Singer and Walsh, 1987; McManus and Magleby, 1988, 1991; Song and Magleby, 1994; Rothberg and Magleby, 1998, 1999). Heterologous expression of Slo α subunits has allowed the combined use of single-channel, macroscopic ionic current and macroscopic gating current measurements to better understand the Slo channel gating behavior (Cox et al., 1997b; Cui et al., 1997; Stefani et al., 1997; Diaz et al., 1998; Horrigan and Aldrich, 1999; Horrigan et al., 1999). Many aspects of voltage- and Ca^{2+}-dependent gating properties of Slo channels have been successfully modeled by allosteric voltage-dependent schemes incorporating probable structural features of the Slo channel, such as the formation of homomultimeric tetramers (Cox et al., 1997a; Horrigan and Aldrich, 1999; Horrigan et al., 1999; Rothberg and Magleby, 1999). However, a full and complete description of the channel gating behavior probably requires a model with additional transitions (Nimigean and Magleby, 1999; Talukder and Aldrich, 2000).

Reactive oxygen/nitrogen species (ROS/RNS) are commonly generated in vivo and implicated in many physiological functions and pathological conditions such as Alzheimer's disease and Parkinson's disease by oxidatively modifying various proteins (Halliwell, 1992; Evans, 1993; Jenner and Olanow, 1996; Markesbery, 1997; Stadtman and Berlett, 1998). ROS/RNS, capable of altering various ion transport mechanisms (Kourie, 1998), are considered to play critical roles in the regulation of vascular tension (Rubanyi, 1988) and also in reperfusion injury (Opie, 1989). Because of their importance in controlling vascular tone (Brayden, 1996; Rusch et al., 1996; Brenner et al., 2000; Pluger et al., 2000), the regulation of BK_{Ca} channels by nitric oxide (NO) has been extensively studied (Beech, 1997; Michelakis et al., 1997). Effects of NO mediated by cGMP-dependent signal transduction pathways are well-known (Southam and Garthwaite, 1996; Vaandrager and de Jonge, 1996; Lohmann et al., 1997). NO (or its related species) may also regulate its physiological effectors by acting as a weak radical, promoting oxidation (Stamler, 1994). In rat pituitary, NO enhances the BK_{Ca} activity in a guanylyl cyclase–independent manner, suggesting that RNS may directly modify the BK_{Ca} protein by acting on sulfhydryl groups (Ahern et al., 1999). Oxidizing agents such as H_2O_2 may induce up- or downregulation of BK_{Ca} channels, depending on the experimental preparation used (Park et al., 1995; Thuringer and Findlay, 1997; Wang et al., 1997; Barlow and White, 1998; Hayabuchi et al., 1998; Brzezinska et al., 2000; Gong et al., 2000). DiChirara and Reinhart (1997) showed that H_2O_2 decreased the activity of the human Slo (*h*Slo) channel by shifting its voltage sensitivity to a more positive direction (Dichiara and Reinhart, 1997). They also showed that rundown of the *h*Slo channel observed on patch excision could be explained by cysteine oxidation, in part, because the reducing agent dithiothreitol (DTT) reversed the effect of patch excision to decrease the channel activity. This redox regulation may contribute to the observed variability in the voltage dependence of heterologously expressed *h*Slo (Stefani et al., 1997) and *m*Slo (Horrigan et al., 1999).

Methionine in proteins is readily oxidized to methionine sulfoxide (met(O)) (Vogt, 1995), which is reduced back to methionine by the enzyme peptide methionine sulfoxide reductase (MSRA) using thioredoxin in vivo or DTT in vitro (Rahman et al., 1992; Moskovitz et al., 1996; Kuschel et al., 1999). Oxidation of methionine to met(O) by the addition of an oxygen atom drastically changes its side chain properties (Black and Mould, 1991). Increasing evidence suggests that reversible oxidation of methionine involving MSRA may function as a general antioxidant mechanism (Levine et al., 1996; Moskovitz et al., 1998) and also as an important physiological regulator of many proteins (Ciorba et al., 1997, 1999; Berlett et al., 1998; Gao et al., 1998; Kuschel et al., 1999; Hoshi and Heinemann, 2001). We showed previously that oxidation of methionine in voltage-dependent *Shaker* potassium channels regulates N-type inactivation (Ciorba et al., 1997) and P/C-type inactivation (Chen et al., 2000). Slowing of N-type inactivation induced by oxidation of a specific methionine residue in the NH_2-terminal ball domain was reversed by overexpression of MSRA (Ciorba et al., 1997; Kuschel et al., 1999). Oxidation of the NH_2-terminal methionine residue was promoted by NO donors and overexpression of nitric oxide synthase, suggesting that methionine oxidation could play a physiologically

important role in the regulation of cellular excitability (Ciorba et al., 1999).

In the present study, we examined whether methionine oxidation regulates the function of *h*Slo channels heterologously expressed in mammalian cells. We show here that oxidation induced by chloramine-T (Ch-T) of methionine shifts the steady-state macroscopic conductance to a more negative direction by accelerating specific voltage-dependent opening transitions and also by slowing the rate limiting closing transition. Our results also suggest that the *h*Slo channel is regulated in an opposing manner by methionine oxidation and cysteine oxidation. This opposing regulation of the *h*Slo channel by cysteine and methionine oxidation contributes to the rundown and run-up of the channel induced by patch excision, and could play important roles in mediating the physiological and pathophysiological effects of ROS/RNS on cellular excitability.

MATERIALS AND METHODS

Channel Expression

Stably Expressed hSlo Channel. The human Slo (U11058; Wallner et al., 1995) channel stably expressed in HEK cells (HF1; Meera et al., 1997) was obtained from the laboratory of Dr. R.W. Aldrich (Stanford University, Stanford, CA). This channel contains a myc tag at the NH_2 terminus, however, its electrophysiological properties are reported to be indistinguishable from those of the wild type *h*Slo channel (Meera et al., 1997). Similar electrophysiological effects of Ch-T were also obtained from HEK and COS cells transiently expressing the *h*Slo channel.

Mutant hSlo Channels. A mutant of the *h*Slo channel (huR2, U11058; Wallner et al., 1995) in which every cysteine was replaced with alanine is referred to here as cys-less *h*Slo and contains the following mutations: C14A, C53A, C54A, C56A, C141A, C277A, C348A, C422A, C430A, C485A, C498A, C554A, C577A, C612A, C615A, C628A, C630A, C695A, C722A, C797A, C800A, C820A, C911A, C975A, C995A, C1001A, C1011A, C1028A, and C1051A. The human clone huR2(+) (Wallner et al., 1995) was subcloned into pCI-neo vector (Promega). The cys-less huR2 DNA was generated by the "overlap extension" technique (Ho et al., 1989; Hirschberg et al., 1995). PCR amplification was carried out using proofreading *Pfu* DNA polymerase. Using the cys-less and wild-type channels, the following chimeric channels were constructed using the overlap extension method (Ho et al., 1989; Hirschberg et al., 1995): chimera No. 0 (C14A, C53A, C54A, C56A, C141A, C277A, C348A, C695A, C722A, C797A, C800A, C820A, C911A, C975A, C995A, C1001A, C1011A, C1028A, C1051A) and chimera No. 1 (C14A, C53A, C54A, C56A, C141A, C277A, C348A, C422A, C430A, C797A, C800A, C820A, C911A, C975A, C995A, C1001A, C1011A, C1028A, and C1051A). The integrity of the constructs was verified by nucleotide sequencing (automated DNA sequencer, ABI 377). The channels were transiently expressed in COS or HEK cells using GenePORTER™ 2 (Gene Therapy Systems). We did not observe any noticeable difference in the channel properties whether they are expressed in COS or HEK cells.

Electrophysiology

The Slo channel currents were recorded in the excised inside-out configuration using an AxoPatch 200A amplifier modified to expand the command voltage range or by an AxoPatch 200B (Axon). The output of the amplifier with the built-in filter set at 10 kHz was digitized using an ITC-16 AD/DA interface attached to an Apple Power Macintosh computer. The data acquisition was controlled by Pulse (HEKA). Linear leak and capacitative currents were subtracted using the *P/n* protocol as implemented in Pulse.

Patch pipets (Warner Instrument Corp.) were coated with dental wax and had a typical initial resistance of 0.8∼1 MΩ in the macroscopic current experiments. For the single-channel experiments, the pipet size was adjusted to obtain a small number of channels. In some experiments with a large number of channels (>10 nA at 180 mV), the series resistance was partially compensated (∼40%); however, in other experiments, the compensation was not routinely employed. The electrophysiological parameter values estimated did not show any systematic correlation with the current amplitude (see legends of Figs. 3 and 5) and suggest that the series resistance error had negligible effects on the results obtained. The experiments were performed at room temperature (20–23°C).

Reagents and Solutions

Both the external and internal solutions contained (in mM): 140 KCl, 2 $MgCl_2$, 11 EGTA, and 10 HEPES, pH 7.2, adjusted with *N*-methyl-D-glucamine. The free Ca^{2+} concentration of this solution was estimated to be <0.4 nM assuming that the residual contaminating Ca^{2+} concentration was 20 μM (Patcher's Power Tools v1.0, F. Mendez; http://www.wavemetrics.com/TechZone/User_ThirdParty/ppt.html) and the ratiometric Fura-2 measurement showed that this solution contained <0.2 nM free Ca^{2+}. In some experiments, $MgCl_2$ was omitted to better study the Ca^{2+} sensitivity of the channel. Other solutions used are noted in the legends.

Chloramine-T (sodium salt), 5,5′-dithio-bis(2-nitrobenzoic acid) (DTNB) and p-chloromercuribenzoic acid (PCMB) were obtained from Sigma-Aldrich. Methanethiosulfonate ethylammonium (MTSEA) was purchased from Toronto Research Chemicals. The experimental solutions containing these reagents were prepared and the pH was adjusted immediately before use. Two types of experimental chambers were used in this study: one with an effective volume of ∼150 μl and the other with an effective volume of ∼500 μl. In those experiments, using the 150-μl chamber, typically Ch-T (four to five times the bath volume) was applied manually using a pipet and then washed out with 1 ml of Ch-T–free solution. The large chamber was continually perfused at 20 μl/s. We did not observe any systematic difference in the efficacy of Ch-T between the two methods. Recombinant bovine MSRA was purified from *Escherichia coli* as described previously (Moskovitz et al., 1996).

Data Analysis

Macroscopic and single-channel current data were analyzed using PulseFit (HEKA), PatchMachine (http://www.hoshi.org), and IgorPro (WaveMetrics) running on Apple Power Macintosh computers. Statistical analysis was carried out using Data Desk (Data Description).

RESULTS

Oxidation by Ch-T Increases hSlo Channel Current

Ch-T is an oxidizing agent that preferentially oxidizes methionine to methionine sulfoxide (met(O)) and it also oxidizes cysteine (Shechter et al., 1975). Selective oxidation of methionine to met(O) by Ch-T (0.5–10 mM) has been demonstrated in different proteins (Shechter et al., 1975; Wang et al., 1985; Beck-Speier et al., 1988; Miles and Smith, 1993; Nedkov et al., 1996; Schlief et al., 1996; Fu et al., 1998; Stief et al., 2000).

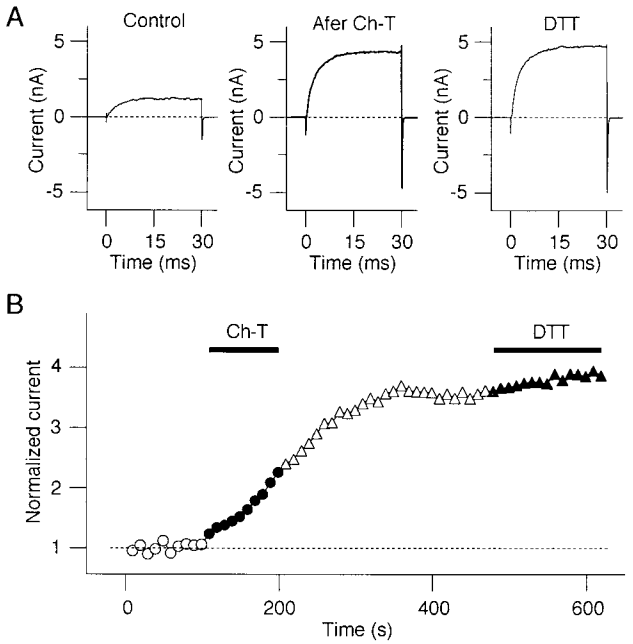

FIGURE 1. Oxidation by Ch-T enhances *h*Slo currents. (A) Representative *h*Slo currents before, after Ch-T treatment, and after DTT application. The currents were elicited in response to pulses from −70 to 130 mV in the inside-out configuration. 2 mM Ch-T was applied for ~1 min and washed out. After washing the chamber for 5 min, 2 mM DTT was applied to the patch. (B) Normalized peak amplitudes of the *h*Slo currents in a representative experiment. The currents were elicited by pulses from −70 to 130 mV every 10 s. At time t = 0, the patch was excised. The current amplitudes were normalized to the average current amplitude during the first 100 s (open circles). 2 mM Ch-T was applied to the cytoplasmic side for 90 s (closed circles) and washed for ~5 min (open triangles). After the wash, 2 mM DTT was applied to the bath (closed triangles).

Ch-T has been reported to modulate inactivation of several ion channels, including voltage-gated Na^+ (Wang et al., 1985; Quinonez et al., 1999) and voltage-gated K^+ channels (Schlief et al., 1996; Stephens et al., 1996; Ciorba et al., 1997), and at least some of these alterations have been attributed to oxidation of methionine residues (Schlief et al., 1996; Ciorba et al., 1997; Quinonez et al., 1999). To examine functional roles of methionine oxidation in the BK_{Ca} channel function, we investigated the effects of Ch-T on *h*Slo channels stably expressed in HEK cells (Meera et al., 1997). Representative macroscopic ionic currents obtained using the inside-out patch-clamp configuration in the virtual absence of $[Ca^{2+}]$ (<0.2 nM) are shown in Fig. 1. With this low internal $[Ca^{2+}]$, the Slo channel essentially acts as a voltage-dependent channel, thus, simplifying the data analysis (Meera et al., 1996; Cui et al., 1997; Horrigan and Aldrich, 1999; Horrigan et al., 1999).

Application of 2 mM Ch-T to the cytoplasmic side in the inside-out configuration markedly increased the currents elicited by depolarization to 130 mV (Fig. 1 A). The peak *h*Slo current amplitude recorded at 130 mV as a function of time in one representative experiment is plotted in Fig. 1 B. In our experimental condition (<0.2 nM Ca^{2+}), the current amplitudes were typically stable for 2–4 min after the patch excision. However, in longer recordings, the Slo macroscopic current amplitudes decreased in some patches (rundown; see Figs. 11 and 12 and also Dichiara and Reinhart, 1997), whereas in other patches they actually increased (run-up; see Figs. 11 and 12). In nearly all of the patches examined, application of Ch-T to the cytoplasmic side gradually increased the peak current amplitudes recorded at 130 mV, usually by 200–300% (see Fig. 3 for statistics).

The effect of Ch-T to increase the *h*Slo current was not dependent on the expression level (see Fig. 3 legend for statistics). Similar effects were also observed when the *h*Slo α subunit alone was heterologously expressed in COS and HEK cells using the transient DNA transfection protocol. Although we cannot totally exclude the possibility that the effect of Ch-T was, in part, mediated by endogenous β subunits present in the cells tested, it is likely that Ch-T altered the Slo α subunit.

The enhanced *h*Slo current caused by Ch-T persisted even after the bath was washed extensively, up to 40 min. This observation is consistent with the idea that the channels were oxidatively modified by Ch-T. Furthermore, subsequent application of the membrane permeable reducing agent DTT (2 mM) to the patch did not reverse the current-enhancing effect of Ch-T (Fig. 1). Application of DTT alone readily reverses the effects of cysteine oxidation in many proteins, including voltage-gated K^+ channels (Ruppersberg et al., 1991; Rettig et al., 1994; Heinemann et al., 1995). Therefore, this observation that application of DTT alone failed to reverse the effect of Ch-T to increase the Slo current amplitude suggests that reversible oxidation of cysteine may not mediate this phenomenon.

We found that the time course of the *h*Slo current increase induced by Ch-T was dependent on the Ch-T concentration used. With 2 mM Ch-T, the maximum current enhancement effect was usually observed within 1–2 min of application. With lower concentrations, the time course of the current enhancement was progressively slower and, with higher concentrations, the modification time course was faster. Because a prolonged incubation of the patch with Ch-T inevitably destroyed the seal, we typically used a brief application period (1–3 min) using 1–5 mM Ch-T to increase the Slo current amplitude and Ch-T was washed out. In the presence of higher concentrations of Ch-T (≥5 mM), a transient decrease in the Slo peak current amplitude was sometimes observed. This transient reduction in the current amplitude is consistent with a fast block of the channel by Na^+ (Yellen, 1984) as Ch-T was applied in the form of Na^+ salt. We did find that 5 mM Na^+ decreased the peak *h*Slo current amplitude by 20–30% (data not shown).

However, we cannot exclude other possibilities such as Ch-T itself acting as an open channel blocker of the channel or Ch-T oxidizing other targets.

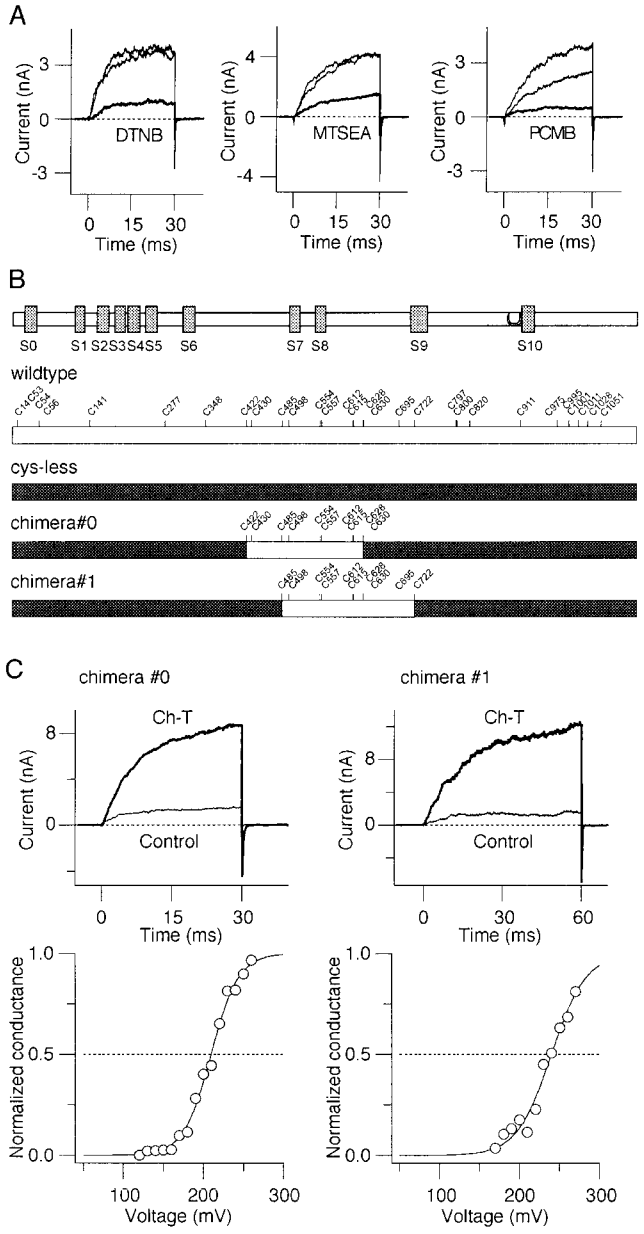

FIGURE 2. Cysteine modification decreases *h*Slo currents. (A) Representative effects of cysteine-specific reagents on wild-type *h*Slo currents. In each panel, the currents in the control condition, after wash-out following application of the cysteine reagent indicated (from left to right: DTNB, MTSEA, and PCMB), and after application of 2 mM DTT are shown. The currents in the left panel (DTNB) were recorded at 150 mV, and those in the middle (MTSEA) and right (PCMB) panels were recorded at 130 mV. The concentrations of DTNB, MTSEA, and PCMB were 1, 0.1, and 0.5 mM, respectively. In each panel, the smallest current represents the result recorded after application of the modifying agent indicated. (B) Schematic diagrams of the structural organizations of the wild-type and mutant *h*Slo channels. The top diagram shows the putative structural organization of the Slo channel according to Wallner et al. (1996). The shaded boxes represent putative helical segments. The wild-type channel (top, open rectangle) contains 29 cysteine residues, and these are replaced with alanine in the cys-less channel (closed rectangle). The cysteine residues that remain in chimera No. 0 are C422, C430, C485, C498, C554, C557, C612, C615, C628, and C630. The following cysteine residues remain in chimera No. 1 C498, C554, C557, C612, C615, C628, C630, C695, and C722. (C) Representative currents from chimera No. 0 (left) and No. 1 (right) expressed in HEK cells recorded before and after treatment with Ch-T (2.5 mM for 1 min, top). Representative macroscopic G-V curves obtained from the two mutant channels are also shown (bottom). The currents from chimera No. 0 (left) and chimera No. 1 (right) were recorded at 180 and 190 mV, respectively. As found with wild-type *h*Slo currents, the deactivation time course was slower after application of Ch-T (see Fig. 5). To determine G-V, the currents were elicited by 50- or 60-ms pulses from −80 mV, and the tail currents were recorded at −90 mV. The curves represent Boltzmann fits to the G-V data (see Fig. 3 legend). The values of $V_{0.5}$ and Q_{app} for chimera No. 0 and No. 1 were 210 mV and 1.4*e*, and 240 mV and 1.2*e*, respectively.

Cysteine-specific Reagents Decrease hSlo Current

While Ch-T may oxidize cysteine in addition to methionine, the above observation that DTT fails to reverse the effect of Ch-T argues against the possibility that reversible cysteine oxidation is involved. To further verify this idea, we examined the effects of cysteine-specific reagents, DTNB (Eyzaguirre, 1987; Shriver et al., 1998), MTSEA (Karlin and Akabas, 1998), and PCMB (Eyzaguirre, 1987; Shriver et al., 1998) on *h*Slo currents. In contrast to the current-enhancing effect of Ch-T, these sulfhydryl reagents all decreased *h*Slo currents in a qualitatively similar manner and application of DTT reversed the effect (Fig. 2 A), arguing that cysteine modification is unlikely to mediate the effect of Ch-T. Our results are consistent with those of Wang et al. (1997) who showed that MTSEA inhibited the opening of native BK_{Ca} channels in smooth muscle cells.

In addition, we also constructed a mutant *h*Slo channel in which all 29 cysteine residues were replaced with alanine (cys-less Slo). Although some *h*Slo-like macroscopic currents that were enhanced by Ch-T were detected in a small number of patches ($n = 4$), the overall expression efficiency in our practical experimental voltage range (up to 250–300 mV) was too poor to study effectively. Thus, we constructed a series of chimeric channels based on the wild-type and cys-less *h*Slo channels. Expression efficacies of the channels with mutations of the cysteine residues in and near the S7, S8, and S9 segments (C498, C554, C557, C612, C615, C628, and C630) were also too low to study in detail in a systematic manner (data not shown). Wood and Vogeli (1997) also reported that C612 may be impor-

tant in the functional expression of the Slo channel in *Xenopus* oocytes using the two-electrode voltage-clamp method (Wood and Vogeli, 1997).

Fig. 2 B shows two of the chimeric channels that could be readily examined electrophysiologically. These two channels in combination contain mutations of 21 out of 29 cysteine residues located in the core and the distal tail domains of the channel (C14, C53, C54, C56, C141, C277, C348, C422, C438, C485, C695, C722, C797, C800, C820, C911, C975, C1001, C1011, C1028, and C1051). Voltage dependence of the two chimeric channels was shifted to a more positive direction by at least 40 mV (compare Fig. 2 C with Fig. 3 D). Application of Ch-T markedly increased the currents through these channels (Fig. 2 C, top) in a manner similar to that observed with the wild-type channel (see Fig. 1). These mutant and cysteine reagent results together suggest that the effect of Ch-T to enhance the *h*Slo current, which is not reversed by DTT, is unlikely to be mediated by reversible oxidation of cysteine.

Ch-T Shifts the Voltage Dependence in the Virtual Absence of Internal Ca^{2+}

Representative *h*Slo currents recorded at different test voltages and the resulting peak current-voltage (I-V) curves obtained before and after Ch-T treatment are compared in Fig. 3. Ch-T increased the current amplitudes especially at slight and moderately depolarized voltages (80–160 mV), and the current-enhancing effect was less noticeable at very positive voltages (>180 mV; Fig. 3). The relative increase in the current amplitude as a function of the test voltage is presented in Fig. 3 C. The graph illustrates the potent effect of Ch-T to increase the *h*Slo channel currents at low and moderate voltages. At low voltages (90–120 mV), Ch-T often increased the current amplitudes by >500%. The voltage dependence shown in Fig. 3 C also confirms that Ch-T became less effective in enhancing the current amplitudes at more positive voltages where the open probability may be nearly saturated. This observation is consistent with the possibility that Ch-T increases the proba-

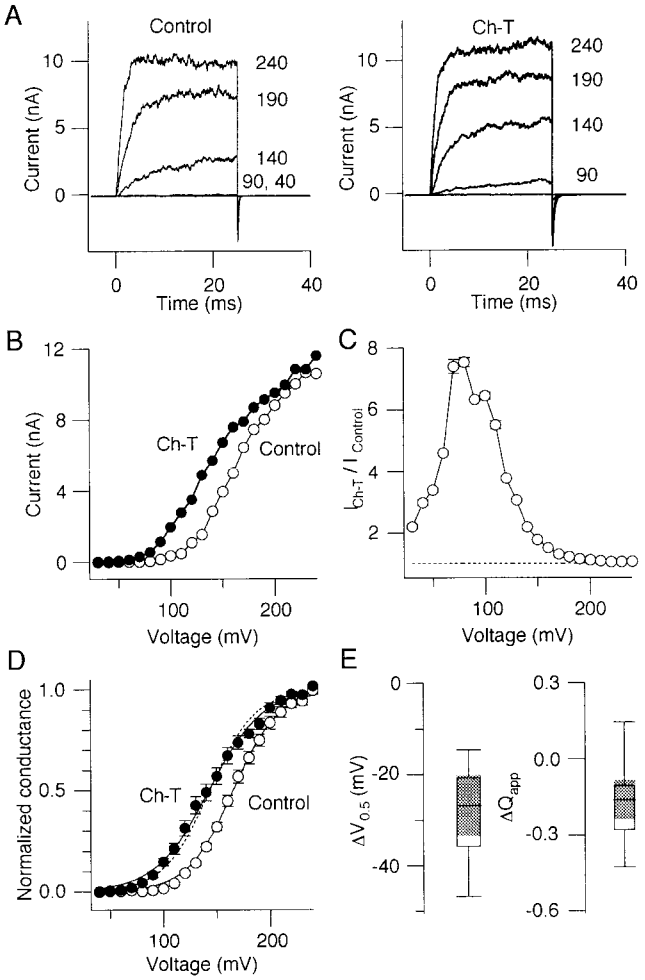

FIGURE 3. Voltage-dependent enhancement of *h*Slo currents by Ch-T. (A) Representative *h*Slo currents elicited in response to pulses to 40, 90, 140, 190, and 240 mV from the holding voltage of −70 mV. 2 mM Ch-T was applied to the patch for 1 min and washed out. (B) Peak I-V curves before and after modification by Ch-T (2 mM for 1 min) in a representative experiment. The results were obtained from the records shown in A. (C) Fractional increase in the peak *h*Slo current amplitude induced by 2 mM Ch-T at different test voltages. At each test voltage, the current amplitude obtained after Ch-T modification was normalized to the pretreatment control current amplitude. The currents were elicited as in A ($n = 13$). (D) Macroscopic G-V curves before and after modification by Ch-T (2 mM for 1 min). The *h*Slo macroscopic currents were elicited by pulses to different test voltages from the holding voltage of −70 mV, and the tail currents were measured at −65 mV in some experiments and at −45 mV in others. We did not see any systematic difference between the results obtained at −65 and −45 mV. The tail currents were fitted with a single exponential, and the extrapolated t = 0 current amplitudes were fitted with a Boltzmann curve. The dates were scaled by the estimated peak amplitude in each experiment such that the maximum value of G-V was unity. The $V_{0.5}$ values for the results obtained before and after Ch-T application were 167 ± 0.7 mV and 138 ± 2.9 mV ($n = 13$). The Q_{app} values before and after Ch-T application were 1.3 ± 0.17*e* and 1.1 ± 0.18*e* ($n = 13$). The dashed curve represents the control G-V shifted along the voltage axis to best match the curve obtained after Ch-T treatment. The mean peak current amplitude at 240 mV in the control condition was 7.0 ± 1.2 nA and the median amplitude was 4.7 nA. The results shown were obtained without any added Mg^{2+}. (E) Boxplots showing the changes in $V_{0.5}$ (left) and Q_{app} (right) involved in the *h*Slo steady-state activation induced by Ch-T. The results presented in D are summarized using boxplots. The shaded regions represent the 95% confidence interval of the median. A negative $\Delta V_{0.5}$ value indicates a shift of G-V leftward along the voltage axis towards a more hyperpolarized direction compared with the control G-V in the same patch. A negative Q_{app} value indicates that Q_{app} decreased compared with the control value in the same experiment. The Pearson product-moment correlation coefficient (r) value between the changes in $V_{0.5}$ and the peak current amplitude at 240 mV (I_{240}) was 0.185. The r value between the changes in Q_{app} and I_{240} was −0.078.

bility of the channel being open (P_o). Normalized macroscopic conductance-voltage (G-V) curves were obtained from the tail current amplitudes and compared in Fig. 3 D. We used a simple Boltzmann function as an operational measure, without any strict mechanistic implication, to describe the overall voltage dependence. The average G-V curve in the control condition was approximated by a simple Boltzmann function with an equivalent charge (Q_{app}) of 1.3*e* (±0.05*e*, n = 13) and the half-activation voltage ($V_{0.5}$) of 167 mV (±0.7 mV, n = 13, range 157–185 mV). After Ch-T treatment, $V_{0.5}$ dramatically shifted leftward by 29 mV to 138 mV (±2.9 mV, n = 13, $\Delta V_{0.5}$ range 15–47 mV; $P \leq 0.0001$ paired t test; Fig. 3 E), showing that at a given voltage, especially at low and moderately positive voltages, the channel is much more likely to be open. The average $\Delta V_{0.5}$ illustrated in Fig. 3 may underestimate the maximum effect of Ch-T because the leftward $V_{0.5}$ shifts as large as 40–50 mV were sometimes observed with higher concentrations of Ch-T (5–10 mM) applied for longer durations (5–10 min). However, these harsh oxidizing treatments markedly increased the seal loss frequency.

The shape of G-V was also altered by Ch-T such that the curve appeared less steep. This effect is particularly more noticeable at very positive voltages (>160 mV) and at low voltages (<120 mV). Consistently, Ch-T treatment significantly decreased Q_{app} on the average by 0.2*e* (15%) from 1.3*e* to 1.1*e* (Fig. 3 E; P = 0.008, n = 13, paired t test).

Ch-T Does Not Change the Reversal Potential

Despite the obvious modification of the macroscopic G-V properties, the apparent reversal potential of the *h*Slo channel as estimated from the tail currents recorded at different voltages was unaltered by Ch-T (Fig. 4). This lack of change in the reversal potential, despite the readily observed shift in G-V (see above), argues against the possibility that Ch-T induced a large voltage shift in the recording system.

The Effect of Ch-T Does Not Require Divalent Ions

Cox et al. (1997a) showed that an allosteric model with 10 states adequately explains the overall voltage-dependent *m*Slo gating modulated by Ca^{2+}. According to this model, the results of Ch-T to enhance the channel activity at a given voltage and to induce a leftward shift in the macroscopic G-V curve could be explained by changes in the voltage-dependent open-closed equilibrium constant (L(V)) and/or the Ca^{2+} dissociation constants for the channel. However, the latter possibility is unlikely because the experiments described so far were conducted at a minimal [Ca^{2+}] (<0.2 nM), and it may be assumed that the channels had essentially no Ca^{2+} ions bound (Horrigan et al., 1999). To further confirm that the action of Ch-T did not depend on the availability of

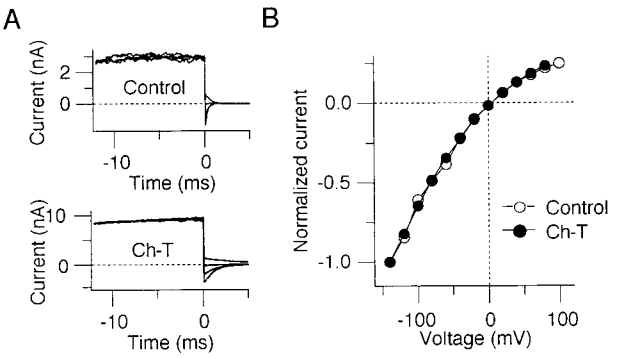

FIGURE 4. Ch-T does not modify instantaneous tail I-V. (A) Representative tail currents recorded at −40,−20, 0, and 20 mV before (top) and after (bottom) Ch-T application (5 mM for 1 min). The currents were elicited by 30-ms pulses from −70 to 130 mV. In the experiment shown, Ch-T increased the current at 130 mV by ~200%. The results shown were obtained without any added Mg^{2+}. (B) Scaled instantaneous tail I-V curves obtained before (open circles) and after (closed circles) Ch-T application (5 mM for 1 min). The tail currents were fitted by a single exponential and the instantaneous (t = 0) currents were estimated by extrapolation. The current amplitudes at different voltages were scaled to the extrapolated tail current amplitudes at −150 mV.

divalent ions, we recorded *h*Slo currents in the presence of 10 mM EDTA without any added Ca^{2+} or Mg^{2+}. We did not observe any noticeable difference in the voltage dependence of the channel activation when the internal solution contained EDTA. Even at these low divalent ion concentrations, Ch-T shifted the G-V curve to a more negative direction and increased the currents recorded at low voltages (data not shown), confirming that the action of Ch-T does not require Ca^{2+} or Mg^{2+}.

Thus, the voltage-dependent open-closed equilibrium constant is the likely target of Ch-T. An allosteric model has been developed to describe the voltage-dependent gating of *m*Slo channel in the virtual absence of Ca^{2+} (Horrigan et al., 1999), and this model can be used as a framework to understand how Ch-T affects the voltage-dependent transitions of *h*Slo channel. To identify the gating transitions modified by Ch-T, we measured the activation and deactivation kinetics at the extreme voltages, which should reflect the rate limiting opening and closing transitions, respectively (Horrigan et al., 1999).

Oxidation by Ch-T Slows the Deactivation Time Course

Application of Ch-T to the cytoplasmic side markedly slowed the kinetics of the *h*Slo tail currents. Representative scaled *h*Slo tail currents recorded at −40 and +40 mV before and after Ch-T treatment are shown in Fig. 5 A. We found that the tail current time course could be approximated by a single exponential at most of the voltages examined (but see Horrigan et al., 1999). The time constant values estimated at different voltages before and after application of Ch-T are plotted in Fig. 5 B. Ch-T increased the time constant of the tail current

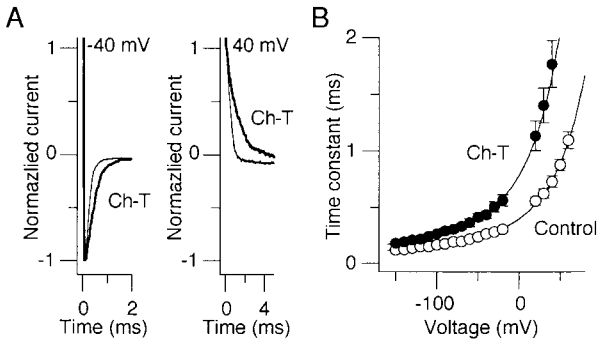

FIGURE 5. Deactivation is slowed by Ch-T. (A) Representative tail currents recorded at −40 mV (left) and 40 mV (right) after 15-ms pulses to 220 mV before and after Ch-T treatment (2 mM for 1 min). In each panel, the tail current recorded after Ch-T treatment (thick sweep) is slower. The results shown were obtained without any added Mg^{2+}. (B) Voltage dependence of deactivation. Tail currents recorded at different voltages were fitted with a single exponential excluding the initial 100 μs. The time constant values estimated before (open circles) and after (closed circles) Ch-T treatment (2 mM, 1 min) are plotted as a function of voltage. At every voltage examined, the time constant value was greater after Ch-T treatment. Voltage dependence of the time constant ($\tau(V)$) was fitted by the equation $\tau_A(0) \cdot \exp(z_A FV/RT) + \tau_B(0) \cdot \exp(z_B FV/RT)$, where $\tau_A(0)$ and $\tau_B(0)$ are the time constant values of the two components at 0 mV, z_A and z_B are their respective equivalent charges, F is Faraday's constant, R is the gas constant, and T is temperature. The values of $\tau_A(0)$ and $\tau_B(0)$ in the control condition were 0.14 ± 0.1 ms and 0.25 ± 0.1 ms. Their respective values after Ch-T treatment were 0.44 ± 0.2 ms and 0.61 ± 0.5 ms. The values of z_A and z_B before Ch-T treatment were 0.12 ± 0.05*e* and 0.77 ± 0.26*e*. After Ch-T treatment, their values were 0.16 ± 0.13*e* and 0.74 ± 0.30*e* (n = 10). The correlation coefficient (r) values between $\tau_A(0)$ and the current amplitude at 240 mV (I_{240}), $\tau_B(0)$ and I_{240}, z_A and I_{240}, and z_B and I_{240} in the control condition were 0.082, −0.41, 0.27, and 0.13, respectively.

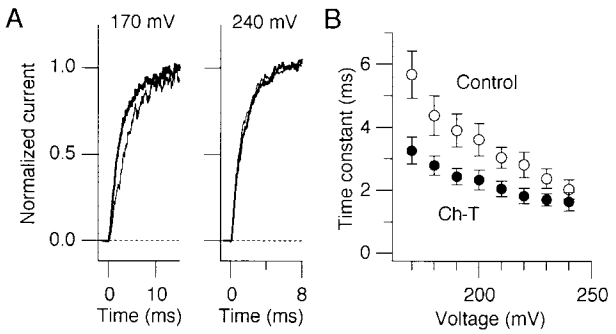

FIGURE 6. Ch-T accelerates activation. (A) Representative currents at 170 mV (left) and 240 mV (right) in response to pulses from the holding voltage of −70 mV. In each panel, the scaled currents obtained before (thin sweep) and after Ch-T treatment (thick sweep, 2 mM for 1 min) are shown. The results shown were obtained without any added Mg^{2+}. (B) Voltage dependence of the activation time constant. The currents were elicited by pulses to different test voltages and the activation time courses excluding the initial 1.5 ms were fitted with a single exponential. The difference in the activation time constant diminishes as the test voltage becomes more positive (n = 12).

at every voltage examined, even at the most negative voltage examined (−150 mV). Horrigan et al. (1999) showed that the voltage dependence of the Slo deactivation time course has two distinct phases, one component with an equivalent charge of 0.52*e* and the other component moving 0.14*e* equivalent charges. Based on their results, we also fitted the voltage dependence of the *h*Slo tail deactivation kinetics, $\tau(V)$, by a sum of two exponential components (Fig. 5B) using the equation $\tau(V) = \tau_A(0) \cdot \exp(z_A FV/RT) + \tau_B(0) \cdot \exp(z_B FV/RT)$, where $\tau_A(0)$ and $\tau_B(0)$ are the time constant values of the two components at 0 mV, z_A and z_B are their respective equivalent charges, F is Faraday's constant, R is the gas constant, and T is the temperature. We found that oxidation by Ch-T specifically increased $\tau_A(0)$ and $\tau_B(0)$ (P = 0.0181, P = 0.0177, respectively, n = 10, paired t test) without significantly affecting their voltage dependence, z_A and z_B (P = 0.262, P = 0.8645, respectively, n = 10, paired t test). The mean values of $\tau_A(0)$ before and after application of Ch-T were 0.25 and 0.44 ms, respectively; and the mean values of $\tau_B(0)$ before and after were 0.14 and 0.61 ms, respectively. If it is assumed that the time constant values estimated at −150 mV reflect the single rate limiting closing transitions (Horrigan et al., 1999), the closing rate constant values before and after Ch-T are calculated to be $8.2 \times 10^3 \pm 4.8 \times 10^2\ s^{-1}$ and $5.5 \times 10^3 \pm 4.1 \times 10^2\ s^{-1}$, respectively.

Ch-T only Slightly Accelerates Activation

In contrast to the marked effect of oxidation by Ch-T to slow the deactivation time course, Ch-T only slightly affected the activation time course of the Slo channel at very positive voltages where the open probability is relatively high. The *h*Slo currents recorded in response to pulses to 170 and 240 mV in the presence of <0.2 nM $[Ca^{2+}]$, before and after treatment with Ch-T, are shown in Fig. 6 A. At 170 mV, where the relative conductance is ~0.6 (Fig. 3), the activation time course was faster after Ch-T treatment (Fig. 6 A, thick, dark sweep). However, at 240 mV, where the relative conductance is near saturation, the activation kinetics was not altered by Ch-T. Except for the initial few hundred microseconds after the depolarization onset, the currents were well described by a single exponential, which is consistent with the earlier observations (Cui et al., 1997; Horrigan et al., 1999). The time constant values estimated before and after Ch-T treatment are plotted as a function of voltage in Fig. 6 B. The results show that the difference in the activation time course observed at less positive voltages disappeared with greater depolarization. At 240 mV, where the open probability is nearly saturated, there was no statistical difference in the activation time constant before and after Ch-T treatment (P = 0.5645, n = 12, paired t test). Since the forward opening transitions dominate at these very pos-

itive voltages, oxidation by Ch-T should have no noticeable effect on the limiting opening transition. Based on the values of the time constant measured, the rate constant value (Horrigan et al., 1999) at 240 mV is estimated to be $\sim$550 s^{-1} (control, 494 $\pm$ 75 s^{-1}; after Ch-T, 606 $\pm$ 72 s^{-1}). In a separate set of experiments, we also verified that Ch-T failed to accelerate the activation time course between 300 and 360 mV ($n = 4$).

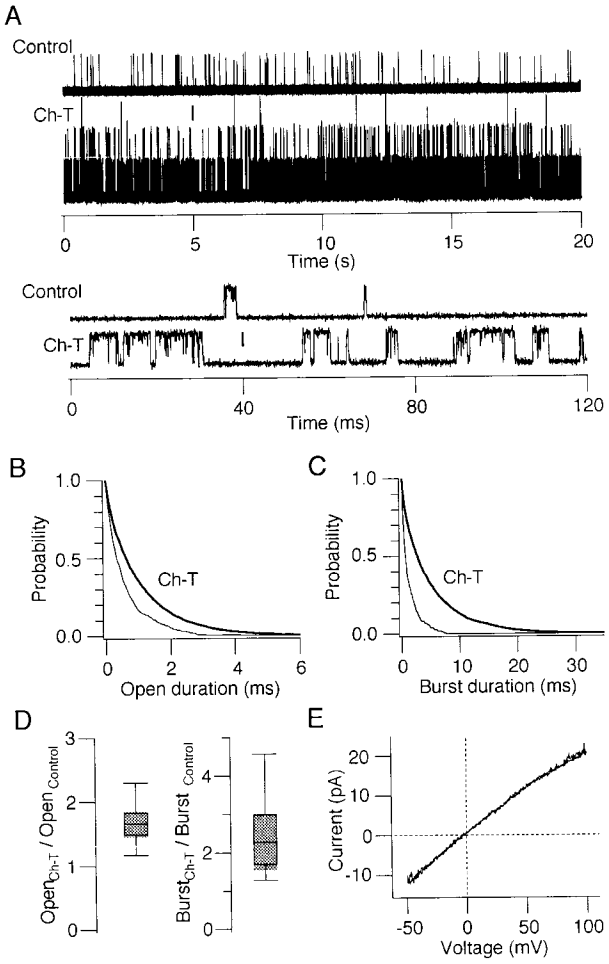

FIGURE 7. Single-channel openings after Ch-T treatment. (A) Representative channel openings at 50 mV before and after Ch-T treatment (2 mM for 1 min). This patch contained at least three channels. The vertical calibration bars represent 5 pA. (B) Open time distributions before (thin curve) and after (thick curve) Ch-T treatment (2 mM for 1 min). The openings were recorded at 50 mV. Each function shows the probability that the open time is greater than the value indicated on the abscissa. The data shown are from the same experiment as shown in A. Only the first-level openings are included in the analysis. Simulations performed using the model presented in the text (also see Fig. 14) suggest that this dwell time analysis method underestimates the mean open and burst durations by <10% for the data containing up to four active channels. (C) Burst duration distributions before (thin curve) and after (thick curve) Ch-T treatment (2 mM for 1 min). The openings were recorded at 50 mV. The first-level openings separated by closed durations shorter than 1 ms were considered to be in the same burst event. Each function shows the probability that the burst duration is greater than the value indicated on the abscissa. The mean values for the burst durations obtained before and after Ch-T treatment were 1.2 and 4.6 ms. The data shown are from the same experiment as shown in A. The error induced by using only the first-level openings is estimated to be <10% using the method described in B. (D) Boxplots summarizing the effects of Ch-T treatment (2 mM for 1 min) on the mean open duration (left) and mean burst duration (right). In each boxplot, the ratios of the mean durations after Ch-T over their respective control values are plotted. The shaded area shows the 95% confidence interval of the median ($n = 9$). (E) Single-channel i-V curves before and after Ch-T treatment. The currents were recorded in response to linear voltage ramps from −50 mV to +100 mV, and then back to −50 mV in 20 ms. 1 mM Ch-T was applied to the cytoplasmic side for 30 s and washed out. The average current amplitude at +100 mV increased by 50% after Ch-T treatment. Although it is possible that not all the channels in the patch were modified by Ch-T, the markedly increased frequency of openings observed at negative voltages suggests that the results were largely obtained from the Ch-T modified channels. The data segments containing open events from 200 data sweeps were manually selected and averaged.

Single-channel Recordings

Single-channel studies show that BK_{Ca} displays bursts of openings with short flicker closures involving multiple dwell time components (Barrett et al., 1982; Methfessel and Boheim, 1982; Moczydlowski and Latorre, 1983; Singer and Walsh, 1987; McManus and Magleby, 1988, 1991; Song and Magleby, 1994; Rothberg and Magleby, 1998, 1999). We investigated the effects of Ch-T on *h*Slo at the single-channel level. Representative single-channel openings recorded in the virtual absence of Ca^{2+} before and after Ch-T application are shown in Fig. 7 using two different time scales. Consistent with the macroscopic results, oxidation by Ch-T enhanced the overall mean current amplitude without obviously affecting the unitary current amplitude (Fig. 7 A).

Open duration histograms obtained from a representative patch are shown in Fig. 7 B. Ch-T increased the mean duration from 0.6 to 1 ms in this experiment, and the open duration distributions were statistically different ($P < 0.01$, Kolmogorov-Smirnov test). The results obtained from multiple experiments show that Ch-T increased the mean open duration typically by 50–100% in a statistically significant manner ($P = 0.0006$, $n = 9$, paired t test; Fig. 7 D). Similarly, the burst distributions shown were also significantly different ($P < 0.01$, Kolmogorov-Smirnov test). Ch-T increased the mean burst duration by 100–200% ($P = 0.006$, $n = 9$, paired t test; Fig. 7, C and D). Thus, the longer open and burst durations at a given voltage contribute to the effect of Ch-T to increase the open probability and lead to greater Slo macroscopic currents.

Single-channel current-voltage (i-V) curves before and after Ch-T treatment were estimated using the ramp voltage protocol (Fig. 7 E). Only the open segments of the ramp current responses were averaged to construct composite open channel i-V curves. The results show that oxidation by Ch-T has no marked effect on the single-channel i-V, supporting the idea that the current-enhancing effect of Ch-T was caused by alterations in the *h*Slo channel gating to increase the open probability. This result is consistent with the observation presented earlier that the macroscopic instantaneous tail currents remained unaltered by Ch-T (Fig. 4).

Ch-T and Ca^{2+} Regulation of hSlo

The results presented above show that Ch-T shifts the voltage dependence of the macroscopic conductance and slows the deactivation kinetics without affecting the limiting activation kinetics in the virtual absence of Ca^{2+} (<0.2 nM). The macroscopic G-V of the Slo channel shifts to more negative voltages with increasing concentrations of Ca^{2+} (Jan and Jan, 1997). We recorded the *h*Slo currents with different internal [Ca^{2+}] to see how much [Ca^{2+}] was required to induce the same amount of shift in $V_{0.5}$ as that caused by Ch-T in the virtual absence of Ca^{2+}. We found that ~300 nM [Ca^{2+}] and Ch-T treatment induced about the same voltage shift in $V_{0.5}$ (Fig. 8, closed symbols). In addition, the time courses of the macroscopic currents recorded in 300 nM [Ca^{2+}] before Ch-T, and in 0.2 nM [Ca^{2+}] after Ch-T were similar (Fig. 8 B). These results suggest that oxidation by Ch-T may mimic almost a 1,000-fold increase in [Ca^{2+}] from 0.2 nM (11 mM EGTA, no added Ca^{2+}) to 300 nM to shift $V_{0.5}$ when α subunits are expressed alone.

Ch-T Fails to Shift $V_{0.5}$ in High [Ca^{2+}] but Reduces Q_{app}

Although the presence of Ca^{2+} is not required for the Ch-T action, we found that the shift in $V_{0.5}$ of G-V produced by Ch-T depended on Ca^{2+}. We recorded the *h*Slo currents in the presence of 0.2 nM (Fig. 9, low Ca^{2+}; 11 mM EGTA, no added Ca^{2+}) and 120 μM Ca^{2+} (Fig. 9, high Ca^{2+}), and examined the effects of Ch-T (Fig. 9). Representative Slo currents elicited at −60 and −20 mV in high Ca^{2+} and those at 120 and 180 mV in low Ca^{2+} are shown in Fig. 9 A. These voltages were selected because the relative conductance values were similar. At both −60 mV in high Ca^{2+} and 120 mV in low Ca^{2+}, the relative macroscopic conductance is ~0.1; and at both −20 mV in high Ca^{2+} and at 180 mV in low Ca^{2+}, the relative conductance is roughly 0.6 (Fig. 9 B). At the voltages where the relative macroscopic conductance is 0.1 (−60 mV in high Ca^{2+} and 120 mV in low Ca^{2+}), oxidation by Ch-T increased the current in high Ca^{2+} by ~100%, whereas in low Ca^{2+}, the current increased by >400%. At the voltages where the relative conductance was 0.6 (−20 mV in high Ca^{2+} and 180 mV in low Ca^{2+}), Ch-T had no obvious effect on the current amplitude in high Ca^{2+}, whereas in low Ca^{2+}, it increased the current by 30%. As presented earlier, Ch-T markedly shifted the G-V curve leftward in low Ca^{2+} (0.2 nM; Fig. 9 B). The mean $V_{0.5}$ values before and after Ch-T treatment in low Ca^{2+} in this set of experiments were 164 and 128 mV ($\Delta V_{0.5}$ = 36 mV), and the difference was statistically significant (P = 0.0008, n = 5, paired t test). In the presence of 120 μM Ca^{2+}, Ch-T did significantly increase the *h*Slo currents at very low voltages (−80 and −60 mV). However, at more positive voltages, Ch-T was much less effective. The $V_{0.5}$ values estimated before and after Ch-T treatment in the presence of 120 μM Ca^{2+} were statically identical (−30 mV, P = 0.95, n = 5, paired t test). These results suggest that gating of the *h*Slo channel with high [Ca^{2+}] in determining $V_{0.5}$ is not as oxidation-sensitive as that with low [Ca^{2+}]. Whether the hSlo channel was treated with Ch-T in the presence of low or high [Ca^{2+}] did not alter the subsequent electrophysiological properties measured after washing Ch-T out of the recoding chamber.

In the presence of high Ca^{2+}, Ch-T did reduce Q_{app} by 0.42e or by 30% (P = 0.0037, n = 5, paired t test). This change in Q_{app} to decrease the steepness of G-V after Ch-T application manifests as greater conductance at low voltages (−80 to −40 mV). For example, Ch-T typically increased the current amplitude by 100% at

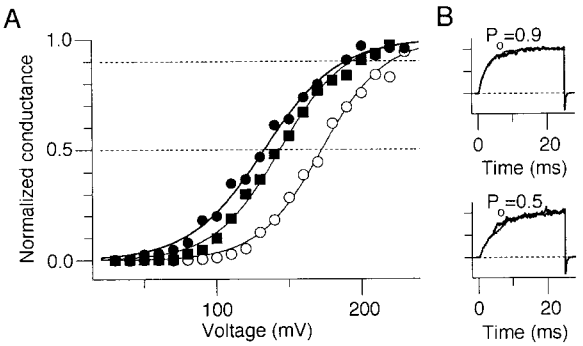

FIGURE 8. $V_{0.5}$ shift induced by Ch-T is mimicked by 300 nM Ca^{2+}. (A) Macroscopic *h*Slo G-V curves were recorded in 0.2 nM [Ca^{2+}] (11 EGTA, no added Ca^{2+}; open circles), 300 nM [Ca^{2+}] (11 mM EGTA, 7 mM Ca^{2+}; squares), and then in 0.2 nM [Ca^{2+}] after Ch-T treatment (2 mM for 1 min; closed circles). The currents were elicited by pulses to different voltages and the tail currents were recorded at −45 mV. The $V_{0.5}$ values for the above conditions were 173, 144, and 133 mV, respectively; the Q_{app} values were 1.15, 1.1, and 0.97, respectively. The results shown were obtained without any added Mg^{2+}. (B) Scaled macroscopic currents recorded at the voltages where the open probability values were 0.9 (top) and 0.5 (bottom). In each comparison, the currents recorded in 300 nM [Ca^{2+}] (thin sweep) and in 0.2 nM [Ca^{2+}] after Ch-T treatment (thick sweep) are shown. For the comparison at P_o = 0.9, the currents recorded at 190 mV in the two conditions are scaled and shown. For the comparison at P_o = 0.5, the current in 300 nM [Ca^{2+}] at 140 mV and the current in 0.2 nM [Ca^{2+}] after Ch-T at 130 mV are scaled and shown.

−60 mV (Fig. 9 A, left) without increasing the currents at more positive voltage where the open probability is higher. This small reduction in Q_{app} is similar to that observed in the low Ca^{2+} condition (Fig. 3 E). Ch-T still slowed the deactivation time course in high Ca^{2+} (Fig. 9 A), even though $V_{0.5}$ was not significantly altered. These observations are consistent with the idea that Ch-T has multiple functional targets.

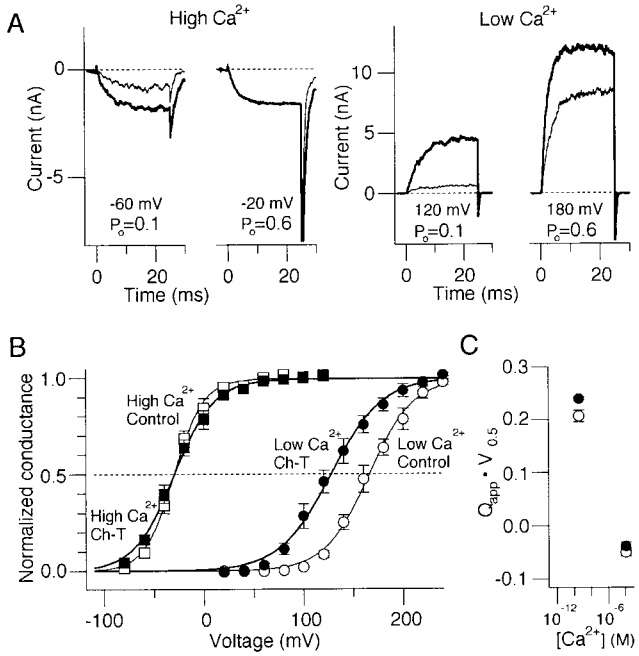

FIGURE 9. High Ca^{2+} attenuates the effect of Ch-T on $V_{0.5}$ but not on Q_{app}. (A) Macroscopic *h*Slo currents recorded in the presence of high Ca^{2+} (120 μM, no EGTA) and low Ca^{2+} (0.2 nM, 11 EGTA, no added Ca^{2+}) before and after Ch-T treatment. In high Ca^{2+}, the data shown were recorded at −60 and −20 mV; in low Ca^{2+}, the data were recorded at 120 and 180 mV. At each voltage, the thick data sweep was obtained after Ch-T. In high Ca^{2+} at −20 mV, the currents before and after Ch-T essentially superimpose. The data sweeps shown are from the same patch. The results were obtained without any added Mg^{2+}. (B) Macroscopic G-V curves before (open symbols) and after (closed symbols) Ch-T treatment (5 mM for 2 min) in the presence of 0.2 nM (circles) and 120 μM (squares) Ca^{2+}. (Open circles) control, low Ca^{2+}; (closed circles) after Ch-T, low Ca^{2+}; (open squares) control, high Ca^{2+}; and (filled squares) after Ch-T, high Ca^{2+}. In each patch, the G-V curves were determined in low and high Ca^{2+}, treated with Ch-T (5 mM for 2 min), and then the G-V curves were measured again in low and high Ca^{2+}. The resulting G-V data were fitted with a Boltzmann function. The values of $V_{0.5}$ in the control/low Ca^{2+}, control/high Ca^{2+}, Ch-T/low Ca^{2+}, and Ch-T/high Ca^{2+} conditions were 161 ± 4, −29 ± 7, 123 ± 7, and −27 ± 4 mV, respectively. The equivalent charges (Q_{app}) estimated in the control/low Ca^{2+}, control/high Ca^{2+}, Ch-T/low Ca^{2+}, and Ch-T/high Ca^{2+} conditions were 1.3 ± 0.1, 1.7 ± 0.2, 1.0 ± 0.04, and 1.2 ± 0.1*e*, respectively (n = 5). (C) Plot of the product of $V_{0.5}$ and Q_{app} as a function of $[Ca^{2+}]$ to infer the mechanism responsible for the apparent overall changes in the Ca^{2+} sensitivity of the channel. The values of $V_{0.5}$ and Q_{app} were estimated as in B.

Cox et al. (1997a) investigated the interaction of voltage and Ca^{2+} in controlling the *m*Slo channel gating and showed that plotting the product of Q_{app} and $V_{0.5}$ as a function of $[Ca^{2+}]$ is a good experimental parameter to examine whether changes in the Ca^{2+} binding affinity or other conformational changes account for the apparent overall changes in the Ca^{2+} sensitivity of the Slo channel. The dependence of the product $Q_{app} \cdot V_{0.5}$ on $[Ca^{2+}]$ before and after Ch-T treatment is shown in Fig. 9 C. Oxidation did not markedly affect the dependence of $Q_{app} \cdot V_{0.5}$ on $[Ca^{2+}]$. According to the formulation of Cox et al. (1997a), the results shown can be interpreted to indicate that Ch-T does not noticeably increase the affinity of Ca^{2+} binding itself, but alters other conformational changes to increase the open probability.

Purified MSRA Partially Reverses the Effect of Ch-T

The observations presented thus far that Ch-T enhanced the *h*Slo current amplitude, that the effect was not reversed by the reducing agent DTT, and that Ch-T enhanced the mutant *h*Slo activity implicate the oxidation of methionine residues. The enzyme peptide methionine sulfoxide reductase (MSRA) specifically reduces met(O) back to methionine using thioredoxin in vivo or DTT in vitro (Moskovitz et al., 1996). MSRA in the presence of DTT has been shown to convert met(O) to methionine in the ShC/B ball peptide and restore fast N-type inactivation (Ciorba et al., 1997). We tested whether MSRA could reverse the effect of Ch-T to enhance the *h*Slo activity by applying recombinant bovine MSRA (Moskovitz et al., 1996) to the cytoplasmic side of the patch (Fig. 10). First, Ch-T was applied to increase the Slo channel activity and the subsequent DTT (2 mM) application did not reverse the effect. However, application of MSRA (15 μg/ml) in the presence of DTT (2-5 mM) gradually decreased the current amplitude, partially reversing the effect of Ch-T. This concentration of DTT is less than optimal for the enzymatic activity in vitro (Moskovitz et al., 1996), however, higher concentrations of DTT almost immediately destroyed the seal in our experimental condition. In addition to the effect on the peak amplitude, MSRA application also accelerated the tail current time course. Similar results were obtained in five other patches. Application of the enzyme alone without any added DTT produced no consistent effect (data now shown; n = 3). It is not clear why we were unable to achieve complete reversal. It is possible that the residues oxidized by Ch-T are not readily accessible by the enzyme. For example, some of the target methionine residues may face the extracellular side. Another possibility, for only the partial reversal, may be that methionine was oxidized by Ch-T to methionine sulfone by the addition of two oxygen atoms. Ch-T oxidizes the methionine residue in the ShC/B ball peptide (Ciorba et al., 1997) to methionine sulfone (Heinemann, S.H., and T. Hoshi,

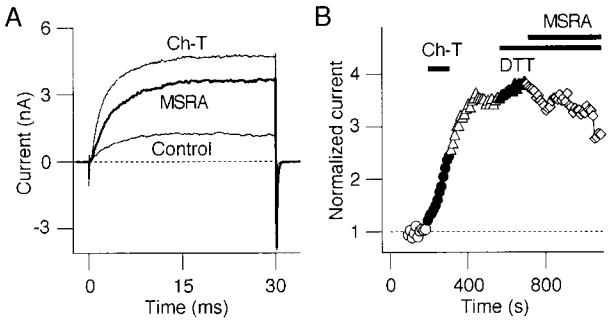

FIGURE 10. MSRA partially reverses the effect of Ch-T. (A) Representative *h*Slo currents in the control condition, after Ch-T application (5 mM for 1.5 min), and after MSRA (15 μg/ml) and DTT application. The currents were elicited by pulses from −70 to 130 mV. (B) Normalized peak current amplitudes recorded in response to a pulse to 130 mV in one representative experiment is plotted as a function of time. Ch-T application (5 mM for 1.5 min) increased the current amplitude by >300%. DTT alone (2 mM) did not affect the current amplitude but MSRA (15 μg/ml) decreased the current amplitude gradually.

unpublished results). MSRA is not effective in reducing methionine sulfone (Eijiri et al., 1979).

The action of MSRA to at least partially reverse the effect of Ch-T further indicates that oxidation of methionine enhances the Slo channel activity. Furthermore, because the enzyme is not likely to cross the membrane from the intracellular side to the extracellular side, the results suggest that at least some of the oxidation and the enzyme target residues must face the cytoplasmic side.

Rundown and Run-up of the Slo Channel

Gating properties of the Slo channel are known to change over time, especially in the excised-patch configuration (Silberberg et al., 1996; Dichiara and Reinhart, 1997). Electrophysiological properties of many other ion channels also change after patch excision, and a variety of biophysical and molecular mechanisms have been proposed to account for these changes (Horn and Korn, 1992; Becq, 1996). Dichiara and Reinhart (1997) showed that the *h*Slo current amplitude decreases with time on patch excision, and that this rundown is prevented by the reducing agent DTT and mimicked by oxidation induced by H_2O_2. They concluded that cysteine oxidation might be involved. We also observed that in some patches, the *h*Slo current amplitude gradually decreased after patch excision (Fig. 11 A). Consistent with the results of Dichiara and Reinhard (1997), we found that H_2O_2 frequently promoted and DTT reversed the channel rundown (data not shown). We also found that DTNB, which preferentially modifies cysteine residues, was effective in decreasing the *h*Slo current amplitude, and this effect was readily reversed by application of the reducing agent DTT (Fig. 11 B; also see Fig. 2). In contrast to the effect of Ch-T, DTNB did not affect the deactivation time course in a consistent way, suggesting that distinct biophysical mechanisms underlie the effects of these oxidizing agents (data not shown).

In other patches, *h*Slo current amplitudes actually increased with time after patch excision (run-up; Fig. 11 C). Based on the foregoing observations, we hypothesized that the increase in the *h*Slo current amplitude after patch excision might involve methionine oxidation. If so, application of MSRA, which catalyzes the reduction of met(O) to methionine, should reverse this effect. In contrast to the effect of DTT on the channel rundown, application of DTT (2 mM) did not alter the increased Slo current amplitude after patch excision (Fig. 11 C). The small increase in the current amplitude seen with the application of DTT may represent a reversal of concurrently occurring rundown mediated by reversible cysteine oxidation (also see Fig. 1 B and Fig. 10 B). The failure of DTT to decrease the current argues against the involvement of cysteine oxidation, which should be easily reversed by DTT (see above). Application of purified MSRA (15 μg/ml) together with DTT (2 mM) to the cytoplasmic side of the patch decreased the run-up Slo current to the initial current level observed immediately after patch excision (Fig. 11 D). Similar observations were obtained in five other macroscopic patches. Thus, spontaneous run-up of *h*Slo induced by patch excision is likely caused by oxidation of methionine residues accessible from the cytoplasmic side. We found that MSRA was noticeably more effective in decreasing the currents which underwent spontaneous run-up after patch excision than the currents enhanced by Ch-T. This is consistent with the possibility that Ch-T may oxidize methionine not only to met(O) but also to methionine sulfone, which is not reduced by MSRA (Eijiri et al., 1979).

The results shown above can be used to explain fluctuations of the macroscopic Slo current amplitude observed in some patches in the excised configuration. Fig. 12 shows the Slo current amplitudes as a function of time after patch excision in three different patches. One patch showed prominent rundown, another patch showed run-up, and the third patch showed slow oscillations in the current amplitude. Out of >140 patches examined in the virtual absence of Ca^{2+} (0.2 nM), the patches that showed rundown and run-up were relatively common, ~50 and 20%, respectively. The patches that exhibited the current fluctuations were much less common (<5%). In the remaining 25%, the current amplitudes were stable. These fluctuations could be considered as a series of rundown and run-up phenomena, which, in turn, could be explained by cysteine and methionine oxidation, respectively.

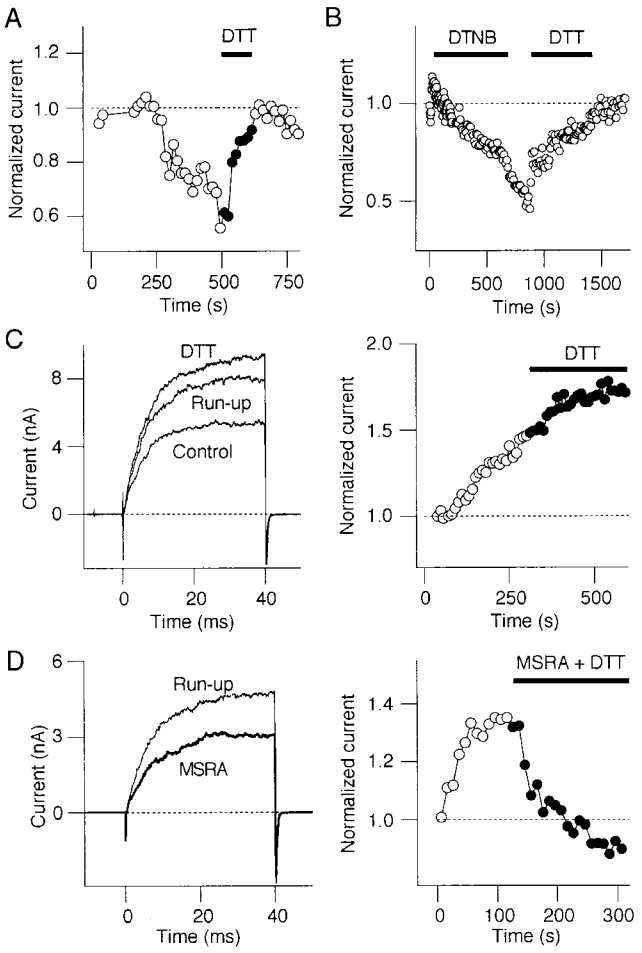

FIGURE 11. Cysteine and methionine oxidation contribute to rundown and run-up. (A) Rundown of the macroscopic *h*Slo current is reversed by the reducing agent DTT. Scaled peak current amplitudes are plotted as a function of time in one representative experiment. The patch was excised at time t = 0. The currents were elicited by pulses to 130 mV. 2 mM DTT was applied to the bath and washed out. (B) DTNB, a cysteine-specific reagent, decreases the *h*Slo current and the effect is reversed by DTT. Normalized peak current amplitudes at 130 mV are plotted as a function of time in one representative experiment. 400 μM DTNB was applied to the bath, washed out, and then 2 mM DTT was applied. The patch was excised at time t = 0. (C) DTT does not reverse the run-up of *h*Slo current. Representative *h*Slo currents recorded immediately after patch excision (control), after run-up (4.5 min after patch excision), and after application of 2 mM DTT in response to pulses to 130 mV are shown superimposed (left). Normalized peak current amplitudes as a function of time are also shown (right). (D) MSRA decreases the spontaneously run-up *h*Slo current. Representative *h*Slo currents recorded at 130 mV after run-up following patch excision (2 min after patch excision) and after 15 μg/ml MSRA and 2 mM DTT are shown superimposed. Normalized peak current amplitudes as a function of time are also shown (right).

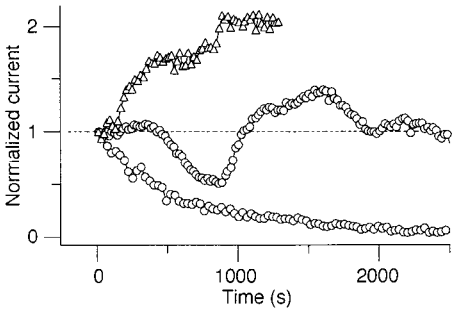

FIGURE 12. Rundown, run-up, and current fluctuations in *h*Slo macroscopic currents. Normalized peak current amplitudes as a function of time in three different patches are shown. The patches were excised at time t = 0 and the currents were elicited by pulses to 130 mV.

Search for Methionine Residues Oxidized by Ch-T

The results presented above suggest that, in the *h*Slo channel-containing patches, oxidation of methionine residues accessible from the cytoplasmic side by Ch-T and at least partially by MSRA enhances the channel activity. The *h*Slo channel contains many methionine residues, especially in the cytoplasmic tail domain, which are thought to contribute to the Ca^{2+} sensitivity of the channel (Wei et al., 1994; Schreiber and Salkoff, 1997; Schreiber et al., 1999). The S5/P/S6 segments of the channel also contain multiple methionine residues. If the methionine residues located within the channel pore are the Ch-T targets, it might be possible to protect the channel from oxidative modification by using the channel blockers that hinder Ch-T's access to the target sites. Therefore, we examined the effect of intracellular TEA on the ability of Ch-T to enhance the *h*Slo channel activity. In *Shaker* voltage-dependent K^+ channels (ShB), M440, T441, and T469 located in or near the pore cavity act as major determinants of internal TEA binding (Yellen et al., 1991; Choi et al., 1993).

The results from a typical experiment using TEA and Ch-T are shown in Fig. 13. The *h*Slo channel is less sensitive to internal TEA than the ShB channel and higher concentrations were necessary to block the channel activity. Application of 80 mM TEA to the cytoplasmic side decreased the macroscopic *h*Slo current at 140 mV to ~10% of the control level. Then, concurrently with TEA, Ch-T was applied to the patch and the channels were incubated in the presence of TEA and Ch-T together for 1.5 min, which is sufficiently long for Ch-T to noticeably increase the *h*Slo current when applied alone (see Fig. 1). In the presence of both TEA and Ch-T, the current amplitude remained at ~10% of the control level, which is consistent with the interpretation that Ch-T did not markedly alter the efficacy of TEA to block the channels. After the concurrent application of TEA and Ch-T together, the bath was washed free of these agents. The *h*Slo current amplitude quickly recovered but only to 10–15% above the control level before the TEA application, and thereafter the current amplitude remained stable. If Ch-T had modified the channels while they were blocked by TEA, the current

amplitude after washing out TEA and Ch-T should have been markedly greater than the control amplitude. The deactivation time course was essentially unchanged during the concurrent application of TEA and Ch-T, and subsequent application of Ch-T alone without TEA slowed the time course. These observations suggest that Ch-T failed to modify the channels while they were blocked by TEA, and are also consistent with the possibility that the channel protein itself is directly oxidized by Ch-T. Subsequent application of Ch-T without TEA progressively increased the *h*Slo current amplitude. Similar results were obtained in six other experiments using TEA. It is not clear why the second Ch-T application without TEA induces only a 40–50% increase in the current amplitude. When applied alone without prior application of TEA, Ch-T often induces a 100–200% increase (Fig. 2). Multiple oxidation targets and their allosteric interactions may be involved. In addition to TEA, we also used another blocker of the *h*Slo channel that works at much lower concentrations (MPTP [1-methyl-4-phenyl-1, 2, 3, 6-tetrahydropyridine], 225 μM; Tang, X.D., and T. Hoshi, manuscript in preparation) and obtained the same results.

Voltage-dependent activation involves conformational changes of ion channel proteins and accessibility/reactivity of the amino acid residues may change during the activation process (Yellen, 1998). Thus, we examined whether the effect of Ch-T to enhance the Slo channel activity was regulated by channel opening/closing by manipulating the holding voltage while the channels were exposed to Ch-T. Keeping the patch at −100 mV without any depolarization or at 130 mV without repolarization at 0.2 nM [Ca^{2+}] did not interfere with the effect of Ch-T to increase the current amplitude.

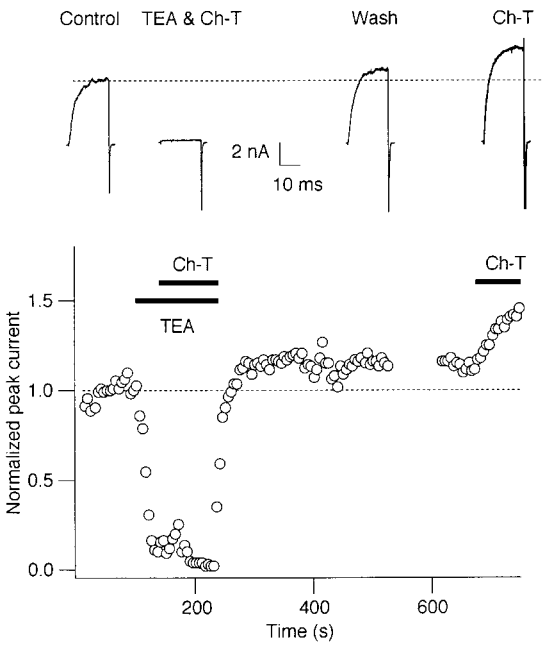

FIGURE 13. Blocked *h*Slo channels are not easily modified by Ch-T. Normalized peak current amplitudes as a function of time in a representative experiment. 80-mM TEA application to the cytoplasmic side reduced the current to a near zero level. 5 mM Ch-T and 80 mM TEA together were then applied. Ch-T did not markedly alter the current amplitude in the presence of TEA. Ch-T and TEA were then washed out and the current amplitude quickly recovered and remained stable. The second application of 5 mM Ch-T gradually increased the current amplitude. The currents were recorded at 140 mV, and representative sweeps are shown at the top. TEA was added to the standard recording solution, and the pH was verified without adjusting the osmolarity. Similar results were obtained using MPTP at 225 μM.

DISCUSSION

Application of oxidizing agents produces multiple effects on the *h*Slo channel. The results presented in this study show that, in the virtual absence of Ca^{2+}, Ch-T increased the Slo channel current by shifting its G-V to a more negative direction by ~30–50 mV. This effect was partially reversed by MSRA and DTT applied together but not by DTT alone. Those reagents that specifically modify cysteine, in contrast, decreased the *h*Slo channel current.

Cysteine Oxidation Decreases hSlo Current

Most naturally occurring amino acids in proteins can be oxidized, however, only the oxidation of cysteine and methionine is readily reversible. Oxidized cysteine is easily reduced back by the reducing agent DTT. For example, N-type inactivation in Kv1.4 and Kv1.4/Kvβ is slowed by oxidation in a cysteine-dependent manner and this effect is readily reversed by DTT (Ruppersberg et al., 1991; Rettig et al., 1994; Heinemann et al., 1995). The observation that the decreased Slo channel current induced by patch excision and H_2O_2 is restored by DTT implicates cysteine oxidation as the underlying mechanism. This conclusion is consistent with the earlier observation of DiChirara and Reinhart (1997). Similarly, DTNB, MTSEA, and PCMB, cysteine-specific reagents, decreased *h*Slo currents and their effects were reversed by DTT.

Methionine Oxidation Increases hSlo Current

Upregulation of the *h*Slo channel activity induced by Ch-T and by patch excision in some experiments is likely to involve methionine oxidation. Our results show that DTT alone does not reverse the increased Slo channel current, but that MSRA applied concurrently with DTT partially reverses the increased current induced by Ch-T or spontaneous run-up, suggesting that oxidation of methionine to met(O) is involved. MSRA specifically reduces met(O) back to methionine using cellular thioredoxin or DTT in vitro (Rahman et al., 1992; Moskovitz et al., 1996). Several possibilities exist to account for the partial but not full recovery obtained with MSRA. Some of the methionine residues could

have been indeed oxidized to methionine sulfone by the addition of two oxygen atoms by Ch-T. MSRA does not reduce methionine sulfone (Eijiri et al., 1979). Another possibility to account for the partial recovery by MSRA is that the oxidized methionine residues may not be easily accessible to the enzyme, as would be the case if they are located near or in the pore cavity. It is also possible that in our experimental condition, the enzyme activity was not sufficiently high (Moskovitz et al., 1996). The observation that all the cysteine-specific reagents we examined decreased the Slo current is consistent with the idea that oxidation of methionine, not cysteine, underlies the effect of Ch-T and run-up. Furthermore, the stimulatory effect of Ch-T is retained in the mutant channels that lack a majority of the cysteine residues (21/29), especially those in the core domain. The robust and consistent effect of Ch-T observed in cell-free excised patches suggests that methionine residues in the *h*Slo channel are directly oxidized to alter the channel gating. Similar effects of Ch-T were observed when *h*Slo was expressed in COS and HEK cells and it is not likely that endogenous β subunits markedly contributed to the phenomena reported here. The finding that internal TEA protects the channel from oxidative modification by Ch-T (Fig. 13) is consistent with the interpretation that the functionally important residues oxidized by Ch-T are located in the channel itself, most likely in the S5/P/S6 segments.

Oxidation of cysteine and methionine, therefore, has opposing effects on the overall Slo channel function. These mechanisms appear to contribute to the rundown, run-up, and current fluctuations of *h*Slo channels observed after patch excision. However, it should be noted other mechanisms could induce similar up- and downregulation of the *h*Slo channel activity, and it is presumptuous to assume that the up- and downregulation of the channel is solely mediated by methionine and cysteine oxidation. Although cysteine and methionine oxidation appear to have opposing overall effects on the *h*Slo channel current, it is not likely that these mechanisms alter the same gating transitions in the opposite directions. Methionine oxidation increases the open probability without markedly affecting the activation time course (this study), whereas cysteine oxidation noticeably slows down the activation time course (Dichiara and Reinhart, 1997).

Biophysical Mechanisms

Several models have been developed to account for gating of BK_{Ca} channels (Horrigan et al., 1999; Nimigean and Magleby, 1999; Talukder and Aldrich, 2000). Here, we have opted to use the model developed by Horrigan et al. (1999; also see their Table I) to account for the observed results of methionine oxidation induced by Ch-T. For the sake of simplicity, the analysis presented here assumes that all the channels measured are homogeneous in terms of the redox state. It is possible that some of the variability observed before application of Ch-T could be explained by differential levels of basal oxidation, thus, violating the homogeneity assumption. This allosteric gating model (referred to here as the HCA model) postulates that the channel operates in an allosteric manner involving five closed (C_0–C_4) and five open states (O_0–O_4) as shown in Scheme 1. The transitions among the

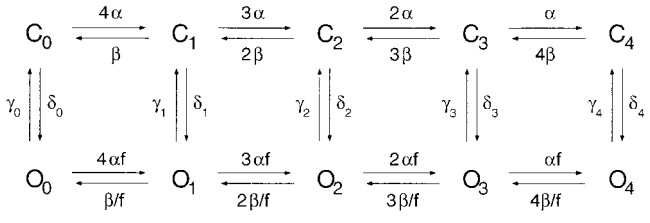

(SCHEME I)

closed and those among the open states (the horizontal transitions in (Horrigan et al., 1999)) are faster and more voltage-dependent than the rate limiting closed-open transitions (the vertical transitions in (Horrigan et al., 1999)). In response to depolarization, the channel may typically proceed from C_0, C_1, C_2, C_3, C_4, and then to O_4. Upon repolarization to a very negative voltage, the channel is likely to close following the O_4-O_3-O_2-O_1-O_0-C_0 pathway. The activation time course at very positive voltages primarily reflects the C_4-O_4 transition, whereas the deactivation time course at negative voltages is mainly determined by the O_0-C_0 transition.

We found that only minor adjustments in the average parameter values in the HCA model at 20°C (Horrigan et al., 1999) were necessary for adequate simulation of the *h*Slo gating behavior in our control condition (<0.2nM Ca^{2+}; see Fig. 14 legend for the parameter values). The value of the closing rate constant γ_0 can be estimated from the deactivation kinetics at −150 mV and the value of the opening rate constant δ_4 from the activation kinetics at 240 mV. The voltage dependence of the rate constants are assumed to be the same as those given in Horrigan et al. (1999) because the voltage dependence of the steady-state macroscopic conductance, the activation kinetics, and deactivation kinetics measured in our study are similar to those obtained by Horrigan et al. (1999). The $\alpha(0)$ and $\beta(0)$ values can be estimated by fitting Eq. 13 in Horrigan et al. (1999) to the measured G-V, assuming that the value of $L(0)$ for *h*Slo is the same as that for *m*Slo.

The parameter values were determined in a similar manner and further adjusted to simulate the effects of Ch-T. The following criteria were used to evaluate the parameter adjustments. First, $V_{0.5}$ shifts to more negative voltages by 30 mV (Fig. 3, D and E). Second, Q_{app} decreases slightly (Fig. 3, D and E). Third, the activation time course at very positive voltages is not accelerated (Fig. 6). Fourth, the deactivation kinetics is slower (Fig.

5). With the values of δ_4 and γ_0 constrained as discussed above, increasing the allosteric factor D shifted $V_{0.5}$, leftward, however, unlike the effect of Ch-T, it also increased Q_{app}. A similar noticeable but small increase in Q_{app} was observed when the ratio $\delta_0(0)/\gamma_0(0)$ was varied to simulate the leftward shift in $V_{0.5}$. These considerations make any alterations in the allosteric factor D or the ratio $\delta_0(0)/\gamma_0(0)$ unlikely to underlie the observed effects of Ch-T. Because changes in δ_0, δ_1, δ_2, and δ_3 do not markedly alter the macroscopic G-V, activation or deactivation kinetics as verified by model simulations, we left these parameters unchanged. With these constraints, we found that acceleration of the C_0-C_1-C_2-C_3-C_4/O_0-O_1-O_2-O_3-O_4 opening transitions (the two horizontal transitions in Horrigan et al. (1999) by increasing the value of α at 0 mV, $\alpha(0)$, by a 2.3-fold ($\Delta\Delta G \approx 2.1$ J/mol) was necessary to simulate the shift in $V_{0.5}$ caused by Ch-T. This simulated shift was also accompanied with a small decrease in Q_{app}. A 60% decrease in the value of the O_0-C_0 transition or γ_0 was required to simulate slowing of the deactivation time course. The C_4-O_4 transition or δ_4 was left unchanged to preserve the activation kinetics at very positive voltages. The *h*Slo macroscopic currents and the G-V curves simulated using the parameter values estimated as described above are shown in Fig. 14. The results nicely meet the four criteria listed above to account for the effects of Ch-T. Although the single-channel properties were not used as the evaluation criteria, the changes in the model parameters well reproduced the increases in the mean open and burst durations observed (data not shown).

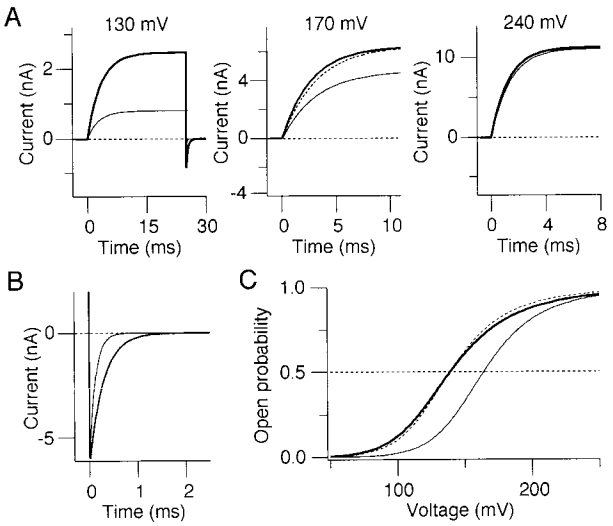

FIGURE 14. Simulation of the Ch-T effects using the HCA model. (A) Ionic currents simulated by the HCA model at 130, 170, and 240 mV. The control *h*Slo currents recorded without any added Mg^{2+} were simulated using the model of Horrigan et al. (1999) with the following parameter values: $\alpha(0) = 1{,}500\ s^{-1}$, $\beta(0) = 35{,}370\ s^{-1}$, $\delta_0(0) = 0.007\ s^{-1}$, $\delta_1(0) = 0.154\ s^{-1}$, $\delta_2(0) = 3.39\ s^{-1}$, $\delta_3(0) = 52\ s^{-1}$, $\delta_4(0) = 65\ s^{-1}$, $D = 22$, $f = D^{0.5}$, $L(0) = \delta_0(0)/\gamma_0(0) = 2 \times 10^{-6}$. The equivalent charge values are as in Horrigan et al. (1999) and they are as follows: $z_\alpha = 0.275e$, $z_\beta = -0.275e$, $z_\delta = 0.262e$, and $z_\gamma = -0.138e$. Each of the simulated channels ($n = 200$) has a linear conductance value of 250 pS and the reversal potential was set at 0 mV. To simulate the effects of Ch-T, the following parameter values were used: $\alpha(0) = 3{,}500\ s^{-1}$, $\delta_0(0) = 0.003\ s^{-1}$, $\delta_1(0) = 0.066\ s^{-1}$, $\delta_2(0) = 1.45\ s^{-1}$, $\delta_3(0) = 52\ s^{-1}$, $\delta_4(0) = 65\ s^{-1}$. In each comparison, the thin data sweep represents the control data sweep and the thick data sweep represents the data after simulated Ch-T. At 170 mV, the simulated control current was scaled up to compare the activation kinetics (dashed line). (B) Simulated tail currents at −150 mV before (thin sweep) and after (thick sweep) simulated Ch-T application. The currents were simulated as in A. (C) Open probability curves as a function of voltage before (thin curve) and after (thick curve) simulated Ch-T application. The data were simulated as in A. The dotted line represents the simulated control curve shifted along the voltage axis to match the simulated Ch-T data.

Interaction with Ca^{2+}

The overall voltage dependence of the *h*Slo channel is regulated by intracellular Ca^{2+} within the dynamic range of 100 nM to 1 mM (Vergara et al., 1998). Ca^{2+} binding is often considered to allosterically modulate the voltage-dependent activation (Cox et al., 1997a; Cui et al., 1997). In the virtual absence of Ca^{2+}, methionine oxidation induced by Ch-T shifts $V_{0.5}$ by 30–50 mV, functionally mimicking the effect of 300–400 nM [Ca^{2+}] (Fig. 8). However, this shift in $V_{0.5}$ by oxidation diminishes in the presence of 120 μM [Ca^{2+}], which is near the high limit of the Ca^{2+} dynamic range of the channel. Although the overall effect of methionine oxidation on $V_{0.5}$ is dependent on [Ca^{2+}], the analysis using the product $V_{0.5} \cdot Q_{app}$ (Cox et al., 1997a) fails to support the idea that oxidation directly alters the Ca^{2+} binding affinity of the channel. Thus, one attractive but speculative idea is that methionine oxidation in the *h*Slo channel partly mimics the influence of the Ca^{2+} binding domain on the voltage-dependent activation mechanism. Even in high [Ca^{2+}], Ch-T does increase the currents at moderately positive voltages by decreasing Q_{app} and slows the deactivation kinetics. This suggests that methionine oxidation may regulate functional roles of BK_{Ca} at a variety of [Ca^{2+}] concentrations.

Molecular Mechanisms

The Slo channel contains a large number of methionine residues and identification of the residues oxidized to bring about the functional effects reported here will require further investigation. However, our results do provide some clues as to where the target residues may be located in the Slo channel. Our simulations using the HCA model show that acceleration of the C_0-C_1-C_2-C_3-C_4/O_0-O_1-O_2-O_3-O_4 opening transitions may underlie the effect of methionine oxidation to shift the voltage dependence of the channel. Horrigan et al. (1999) suggest that these opening transitions may represent

the activation of voltage sensors. Given this interpretation, it could be speculated that methionine residues in the S4/S4–S5 linker segments may be involved. However, the *h*Slo and *m*Slo channels do not contain any methionine residue in these segments and the target residues are likely located elsewhere. The result that the intracellular channel blockers protect the Slo channel from functional modification by Ch-T suggests that the target residues may lie near the channel pore. Because MSRA at least partly reverses the effect of Ch-T, the targets must be accessible from the cytoplasmic side and the residues located deep in the pore can be excluded from consideration. In *Shaker* channels, the PVP motif in the S6 segment may introduce a sharp bend in the S6 segment such that those residues located downstream of this motif may be well exposed to the cytoplasmic side (Durell and Guy, 1992; del Camino et al., 2000). In *h*Slo and *m*Slo channels, the sequence PVP is replaced with YVP, and it is not clear whether a similar arrangement exists. If it does, the methionine residues located near or carboxyl to the YVP motif are the prime oxidation targets. In the simulation presented above, the values of two rate constants in the HCA model, $\alpha(0)$ and $\gamma_0(0)$, were adjusted to account for the shift in $V_{0.5}$, reduced Q_{app} and slowing of the deactivation kinetics. It is not clear at present whether oxidation of a single methionine residue or multiple residues accounts for the required changes in the two rate constants. One scenario that needs to be considered is that for Ch-T to alter the channel function, oxidation of multiple residues in series is required. Ch-T may oxidize one residue, which increases the likelihood of the second residue becoming oxidized, perhaps by increasing the accessibility. The alterations in the multiple rate constants required to adequately simulate the results may reflect this possible sequential nature of the modification process. This mechanism may also explain why the current amplitude continued to increase even after Ch-T was washed out in some experiments (Fig. 1 B).

Taken together, the following tentative model of the action of methionine oxidation to facilitate the Slo channel opening may be proposed. It may be argued that the critical methionine residues in the pore/S6 segments, which are exposed to the cytoplasmic side but sheltered when an intracellular pore blocker is present, are involved in integrating the information from the voltage sensors and the Ca^{2+} binding domain, contributing to regulation of the activation gate. Oxidation of these methionine residues to met(O) by the addition of an extra oxygen atom to the sulfur atom stiffens the side chain and renders it markedly more polar. The hydrophilicity of met(O) has been estimated to be similar to that of lysine (Black and Mould, 1991). This change in the side chain property may partially open the activation gate, likely to be comprised in part by the residues in the S6 segment (Liu et al., 1997; del Camino et al., 2000), and by twisting the S6 segment, as shown for the inner TM2 helices in the KcsA channel (Perozo et al., 1999). This partial opening or potential twisting of the S6 segment primes the activation gate for opening, and it is equivalent to 30–50 mV depolarization ($\Delta\Delta G \approx 2.1$ J/mol) or increasing $[Ca^{2+}]$ from 0.2 to 300 nM.

Possible Physiological Implications

Ca^{2+}-dependent K^+ channels play multitudes of physiological roles, ranging from cochlear frequency tuning (Fettiplace and Fuchs, 1999; Ramanathan et al., 1999) to vascular tone control (Brayden, 1996; Rusch et al., 1996; Brenner et al., 2000; Pluger et al., 2000). Free radicals, such as hydroxyl radicals, capable of promoting oxidation of amino acids are also implicated in vascular regulation (Rubanyi, 1988). NO, an important regulator of blood vessel function (Drexler, 1999; Zanzinger, 1999; Sanders et al., 2000), is a weak radical and may directly or indirectly promote oxidation (Stamler, 1994). Ciorba et al. (1999) showed that NO could promote methionine oxidation in *Shaker* channels, and it would be interesting to see if NO could increase *h*Slo currents. Some studies have shown that application of oxidizing agents increased the BK_{Ca} channel activity (Thuringer and Findlay, 1997; Barlow and White, 1998; Hayabuchi et al., 1998; Gong et al., 2000), whereas others have shown inhibition (Dichiara and Reinhart, 1997; Wang et al., 1997; Brzezinska et al., 2000). Especially in intact cells, it is difficult to predict whether application of oxidizing agents will increase or decrease the BK_{Ca} channel activity. Oxidation may have direct effects on the channel protein mediated by oxidation of its amino acid residues and also indirect effects mediated by oxidation of other molecules, such as those involved in intracellular Ca^{2+} homeostasis (Suzuki et al., 1997; Kourie, 1998; Chakraborti et al., 1999). The presence of β subunits in some, but not all, Ca^{2+}-dependent K^+ channel complexes further contributes to the complexity (Chang et al., 1997; Tanaka et al., 1997; Wanner et al., 1999). For example, in our study, DTNB, like other cysteine-specific reagents examined, decreased the *h*Slo current, whereas native rat hippocampal BK_{Ca} currents were enhanced by DTNB and reversed by DTT (Gong et al., 2000). Even considering only the direct action on the channel protein itself, the effects of oxidation could be complex since there may be multiple oxidation targets, most likely cysteine and methionine residues. The results presented here show that, in the heterologously expressed Slo channel, cysteine oxidation generally inhibits, whereas methionine oxidation enhances the BK_{Ca} channel activity. It will be interesting to know the relative efficacies of cysteine and methionine oxidation in vivo.

Unlike some other regulatory molecules such as protein kinases, ROS/RNS, capable of oxidizing amino acid residues, do not have specific target amino acid consensus sequences for their action and the potential specificity of their action may be conferred by other mechanisms. Possible colocalization of the molecules that generate ROS/RNS with the target molecules and the availability of cofactors, such as Fe, may contribute to the potential specificity.

Clinically, the results presented here may be relevant to reperfusion injury. During reperfusion after an ischemic episode, a burst of free radicals is produced, promoting oxidation of amino acids (Babbs, 1988; Rubanyi, 1988; Gress, 1994). Vascular BK_{Ca} channels may be oxidatively modified during reperfusion. Methionine oxidation of BK_{Ca} channels, which facilitate repolarization to restrict excess Ca^{2+} entry, may serve as a neuronal protective mechanism. Aberrant elevations in intracellular Ca^{2+} and ROS/RNS also have been documented in aged animals and some neurodegenerative diseases (Olanow and Arendash, 1994). When the enhanced BK_{Ca} channel activity is no longer desired, MSRA could decrease the channel function by reducing met(O) to methionine. It is interesting to note that a decrease in the MSRA activity was reported in the Alzheimer's disease brain (Gabbita et al., 1999), which involves increased oxidative stress (Markesbery, 1997). Therefore, methionine oxidation and MSRA could function as a reversible cellular regulatory mechanism.

In summary, we showed here that Ch-T via methionine oxidation increases the *h*Slo Ca^{2+}-dependent K^+ channel activity and that methionine oxidation and cysteine oxidation have opposing effects on the channel activity. We suggest that methionine oxidation may have a role in integration of the information from the voltage sensors and the Ca^{2+} binding domain of the channel. Considering that ROS/RNS production is closely linked to cellular metabolism, reversible regulation of the Slo channel by methionine oxidation and MSRA may represent an important functional coupling mechanism between cellular metabolism and electrical excitability.

We thank C. Schinstock for technical assistance, Dr. Yermolaieva for the fura-2 Ca^{2+} measurement, Drs. V. Avdonin and E. Shibata for discussion and reading of the manuscript, and H. Sumlin for encouragement.

This study was supported in part by the National Institutes of Health grants GM57654 and HL14388 (to T. Hoshi).

Submitted: 4 August 2000
Revised: 17 January 2001
Accepted: 18 January 2001

REFERENCES

Adelman, J.P., K.Z. Shen, M.P. Kavanaugh, R.A. Warren, Y.N. Wu, A. Lagrutta, C.T. Bond, and R.A. North. 1992. Calcium-activated potassium channels expressed from cloned complementary DNAs. *Neuron.* 9:209–216.

Ahern, G.P., S.F. Hsu, and M.B. Jackson. 1999. Direct actions of nitric oxide on rat neurohypophysial K^+ channels. *J. Physiol.* 520: 165–176.

Atkinson, N.S., G.A. Robertson, and B. Ganetzky. 1991. A component of calcium-activated potassium channels encoded by the *Drosophila slo* locus. *Science.* 253:551–555.

Atkinson, N.S., R. Brenner, R.A. Bohm, J.Y. Yu, and J.L. Wilbur. 1998. Behavioral and electrophysiological analysis of Ca-activated K-channel transgenes in *Drosophila. Annu. NY Acad. Sci.* 860:296–305.

Babbs, C.F. 1988. Reperfusion injury of postischemic tissues. *Annu. Emerg. Med.* 17:1148–1157.

Barlow, R.S., and R.E. White. 1998. Hydrogen peroxide relaxes porcine coronary arteries by stimulating BK_{Ca} channel activity. *Am. J. Physiol.* 275:H1283–H1289.

Barrett, J.N., K.L. Magleby, and B.S. Pallotta. 1982. Properties of single calcium-activated potassium channels in cultured rat muscle. *J. Physiol.* 331:211–230.

Beck-Speier, I., L. Leuschel, G. Luippold, and K.L. Maier. 1988. Proteins released from stimulated neutrophils contain very high levels of oxidized methionine. *FEBS Lett.* 227:1–4.

Becq, F. 1996. Ionic channel rundown in excised membrane patches. *Biochim. Biophys. Acta.* 1286:53–63.

Beech, D.J. 1997. Actions of neurotransmitters and other messengers on Ca^{2+} channels and K^+ channels in smooth muscle cells. *Pharmacol. Ther.* 73:91–119.

Berlett, B.S., R.L. Levine, and E.R. Stadtman. 1998. Carbon dioxide stimulates peroxynitrite-mediated nitration of tyrosine residues and inhibits oxidation of methionine residues of glutamine synthetase — both modifications mimic effects of adenylylation. *Proc. Natl. Acad. Sci. USA.* 95:2784–2789.

Black, S.D., and D.R. Mould. 1991. Development of hydrophobicity parameters to analyze proteins which bear post- or cotranslational modifications. *Anal. Biochem.* 193:72–82.

Brayden, J.E. 1996. Potassium channels in vascular smooth muscle. *Clin. Exp. Pharmacol. Physiol.* 23:1069–1076.

Brenner, R., G.J. Perez, A.D. Bonev, D.M. Eckman, J.C. Kosek, S.W. Wiler, A.J. Patterson, M.T. Nelson, and R.W. Aldrich. 2000. Vasoregulation by the beta1 subunit of the calcium-activated potassium channel. *Nature.* 407:870–876.

Brzezinska, A.K., D. Gebremedhin, W.M. Chilian, B. Kalyanaraman, and S.J. Elliott. 2000. Peroxynitrite reversibly inhibits Ca^{2+}-activated K^+ channels in rat cerebral artery smooth muscle cells. *Am. J. Physiol.* 278:H1883–H1890.

Chakraborti, T., S. Das, M. Mondal, S. Roychoudhury, and S. Chakraborti. 1999. Oxidant, mitochondria and calcium: an overview. *Cell Signal.* 11:77–85.

Chang, C.P., S.I. Dworetzky, J. Wang, and M.E. Goldstein. 1997. Differential expression of the alpha and beta subunits of the large-conductance calcium-activated potassium channel: implication for channel diversity. *Brain Res.* 45:33–40.

Chen, J., V. Avdonin, M.A. Ciorba, S.H. Heinemann, and T. Hoshi. 2000. Acceleration of P/C-type inactivation in voltage-gated K^+ channels by methionine oxidation. *Biophys. J.* 78:174–187.

Choi, K.L., C. Mossman, J. Aube, and G. Yellen. 1993. The internal quaternary ammonium receptor site of *Shaker* potassium channels. *Neuron.* 10:533–541.

Ciorba, M.A., S.H. Heinemann, H. Weissbach, N. Brot, and T. Hoshi. 1997. Modulation of potassium channel function by methionine oxidation and reduction. *Proc. Natl. Acad. Sci. USA.* 94: 9932–9937.

Ciorba, M.A., S.H. Heinemann, H. Weissbach, N. Brot, and T. Hoshi. 1999. Regulation of voltage-dependent K^+ channels by methionine oxidation: effect of nitric oxide and vitamin C. *FEBS Lett.* 442:48–52.

Cox, D.H., J. Cui, and R.W. Aldrich. 1997a. Allosteric gating of a

large conductance Ca-activated K^+ channel. *J. Gen. Physiol.* 110: 257–281.

Cox, D.H., J. Cui, and R.W. Aldrich. 1997b. Separation of gating properties from permeation and block in *mslo* large conductance Ca-activated K^+ channels. *J. Gen. Physiol.* 109:633–646.

Cui, J., D.H. Cox, and R.W. Aldrich. 1997. Intrinsic voltage dependence and Ca^{2+} regulation of *mslo* large conductance Ca-activated K^+ channels. *J. Gen. Physiol.* 109:647–673.

del Camino, D., M. Holmgren, Y. Liu, and G. Yellen. 2000. Blocker protection in the pore of a voltage-gated K^+ channel and its structural implications. *Nature.* 403:321–325.

Diaz, L., P. Meera, J. Amigo, E. Stefani, O. Alvarez, L. Toro, and R. Latorre. 1998. Role of the S4 segment in a voltage-dependent calcium-sensitive potassium (hSlo) channel. *J. Biol. Chem.* 273: 32430–32436.

Dichiara, T.J., and P.H. Reinhart. 1997. Redox modulation of hslo Ca^{2+}-activated K^+ channels. *J. Neurosci.* 17:4942–4955.

Drexler, H. 1999. Nitric oxide and coronary endothelial dysfunction in humans. *Cardiovasc. Res.* 43:572–579.

Durell, S.R., and H.R. Guy. 1992. Atomic scale structure and functional models of voltage-gated potassium channels. *Biophys. J.* 62: 238–247.

Eijiri, S.-I., H. Weissbach, and N. Brot. 1979. Reduction of methionine sulfoxide to methionine by *Escherichia coli*. *J. Bacteriol.* 139: 161–164.

Evans, P.H. 1993. Free radicals in brain metabolism and pathology. *Br. Med. Bul.* 49:577–587.

Eyzaguirre, J. 1987. The use of group-specific reagents. *In* Chemical Modification of Enzymes: An Overview. J. Eyzaguirre, editor. John Wiley, New York. 9–22.

Fettiplace, R., and P.A. Fuchs. 1999. Mechanisms of hair cell tuning. *Annu. Rev. Physiol.* 61:809–834.

Fu, Q., P. McPhie, and D.C. Gowda. 1998. Methionine modification impairs the C5-cleavage function of cobra venom factor-dependent C3/C5 convertase. *Biochem. Mol. Biol. Int.* 45:133–144.

Gabbita, S.P., M.Y. Aksenov, M.A. Lovell, and W.R. Markesbery. 1999. Decrease in peptide methionine sulfoxide reductase in Alzheimer's disease brain. *J. Neurochem.* 73:1660–1666.

Gao, J., D.H. Yin, Y.H. Yao, H.Y. Sun, Z.H. Qin, C. Schoneich, T.D. Williams, and T.C. Squier. 1998. Loss of conformational stability in calmodulin upon methionine oxidation. *Biophys. J.* 74:1115–1134.

Gong, L., T.M. Gao, H. Huang, and Z. Tong. 2000. Redox modulation of large conductance calcium-activated potassium channels in CA1 pyramidal neurons from adult rat hippocampus. *Neurosci. Lett.* 286:191–194.

Gress, D.R. 1994. Stroke. Revolution in therapy. *West J. Med.* 161: 288–291.

Halliwell, B. 1992. Reactive oxygen species and the central nervous system. *J. Neurochem.* 59:1609–1623.

Hayabuchi, Y., Y. Nakaya, S. Matsuoka, and Y. Kuroda. 1998. Hydrogen peroxide-induced vascular relaxation in porcine coronary arteries is mediated by Ca^{2+}-activated K^+ channels. *Heart Vessels.* 13:9–17.

Heinemann, S.H., J. Rettig, F. Wunder, and O. Pongs. 1995. Molecular and functional characterization of a rat brain Kvβ 3 potassium channel subunit. *FEBS Lett.* 377:383–389.

Hirschberg, B., A. Rovner, M. Lieberman, and J. Patlak. 1995. Transfer of twelve charges is needed to open skeletal muscle Na^+ channels. *J. Gen. Physiol.* 106:1053–1068.

Ho, S.N., H.D. Hunt, R.M. Horton, J.K. Pullen, and L.R. Pease. 1989. Site-directed mutagenesis by overlap extension using the polymerase chain reaction. *Gene.* 77:51–59.

Horn, R., and S.J. Korn. 1992. Prevention of rundown in electrophysiological recording. *Methods Enzymol.* 207:149–155.

Horrigan, F.T., and R.W. Aldrich. 1999. Allosteric voltage gating of potassium channels II. *m*Slo channel gating charge movement in the absence of Ca^{2+}. *J. Gen. Physiol.* 114:305–336.

Horrigan, F.T., J. Cui, and R.W. Aldrich. 1999. Allosteric voltage gating of potassium channels I. *m*Slo ionic currents in the absence of Ca^{2+}. *J. Gen. Physiol.* 114:277–304.

Hoshi, T., and S.H. Heinemann. 2001. Regulation of cell function by methionine oxidation and reduction. *J. Physiol.* 531:1–11.

Jan, L.Y., and Y.N. Jan. 1997. Ways and means for left shifts in the MaxiK channel. *Proc. Natl. Acad. Sci. USA.* 94:13383–13385.

Jenner, P., and C.W. Olanow. 1996. Oxidative stress and the pathogenesis of Parkinson's disease. *Neurology.* 47:S161–S170.

Kaczorowski, G.J., H.G. Knaus, R.J. Leonard, O.B. McManus, and M.L. Garcia. 1996. High-conductance calcium-activated potassium channels: structure, pharmacology, and function. *J. Bioenerg. Biomembr.* 28:255–267.

Karlin, A., and M.H. Akabas. 1998. Substituted-cysteine accessibility method. *Methods Enzymol.* 293:123–145.

Kourie, J.I. 1998. Interaction of reactive oxygen species with ion transport mechanisms. *Am. J. Physiol.* 275:C1–C24.

Kuschel, L., A. Hansel, R. Schönherr, H. Weissbach, N. Brot, T. Hoshi, and S.H. Heinemann. 1999. Molecular cloning and functional expression of a human peptide methionine sulfoxide reductase (hMsrA). *FEBS Lett.* 456:17–21.

Latorre, R., R. Coronado, and C. Vergara. 1984. K^+ channels gated by voltage and ions. *Annu. Rev. Physiol.* 485–495.

Levine, R.L., L. Mosoni, B.S. Berlett, and E.R. Stadtman. 1996. Methionine residues as endogenous antioxidants in proteins. *Proc. Natl. Acad. Sci. USA.* 93:15036–15040.

Lingle, C.J., C.R. Solaro, M. Prakriya, and J.P. Ding. 1996. Calcium-activated potassium channels in adrenal chromaffin cells. *Ion channels.* 4:261–301.

Liu, Y., M. Holmgren, M.E. Jurman, and G. Yellen. 1997. Gated access to the pore of a voltage-dependent K^+ channel. *Neuron.* 19: 175–184.

Lohmann, S.M., A.B. Vaandrager, A. Smolenski, U. Walter, and H.R. De Jonge. 1997. Distinct and specific functions of cGMP-dependent protein kinases. *Trends Biochem. Sci.* 22:307–312.

Markesbery, W.R. 1997. Oxidative stress hypothesis in Alzheimer's disease. *Free Radic. Biol. Med.* 23:134–147.

Marty, A. 1989. The physiological role of calcium-dependent channels. *Trends Neurosci.* 12:420–424.

McManus, O.B. 1991. Calcium-activated potassium channels: regulation by calcium. *J. Bioenerg. Biomembr.* 23:537–560.

McManus, O.B., and K.L. Magleby. 1988. Kinetic states and modes of single large-conductance calcium-activated potassium channels in cultured rat skeletal muscle. *J. Physiol.* 402:79–120.

McManus, O.B., and K.L. Magleby. 1991. Accounting for the Ca^{2+}-dependent kinetics of single large-conductance Ca^{2+}-activated K^+ channels in rat skeletal muscle. *J. Physiol.* 443:739–777.

Meera, P., M. Wallner, Z. Jiang, and L. Toro. 1996. A calcium switch for the functional coupling between alpha (hslo) and beta subunits (KV, Ca beta) of maxi K channels. *FEBS Lett.* 382:84–88.

Meera, P., M. Wallner, M. Song, and L. Toro. 1997. Large conductance voltage- and calcium-dependent K^+ channel, a distinct member of voltage-dependent ion channels with seven N-terminal transmembrane segments (S0-S6), an extracellular N terminus, and an intracellular (S9-S10) C terminus. *Proc. Natl. Acad. Sci. USA.* 94:14066–14071.

Methfessel, C., and G. Boheim. 1982. The gating of single calcium-dependent potassium channels is described by an activation/blockade mechanism. *Biophys. Struct. Mech.* 9:35–60.

Michelakis, E.D., H.L. Reeve, J.M. Huang, S. Tolarova, D.P. Nelson, E.K. Weir, and S.L. Archer. 1997. Potassium channel diversity in vascular smooth muscle cells. *Can. J. Physiol. Pharmacol.* 75:889–897.

Miles, A.M., and R.L. Smith. 1993. Functional methionines in the col-

lagen/gelatin binding domain of plasma fibronectin: effects of chemical modification by chloramine T. *Biochemistry.* 32:8168–8178.

Moczydlowski, E., and R. Latorre. 1983. Gating kinetics of Ca^{2+}-activated K^+ channels from rat muscle incorporated into planar lipid bilayers. Evidence for two voltage-dependent Ca^{2+} binding reactions. *J. Gen. Physiol.* 82:511–542.

Moskovitz, J., E. Flescher, B.S. Berlett, J. Azare, J.M. Poston, and E.R. Stadtman. 1998. Overexpression of peptide-methionine sulfoxide reductase in *Saccharomyces cerevisiae* and human T cells provides them with high resistance to oxidative stress. *Proc. Natl. Acad. Sci. USA.* 95:14071–14075.

Moskovitz, J., H. Weissbach, and N. Brot. 1996. Cloning and expression of a mammalian gene involved in the reduction of methionine sulfoxide residues in proteins. *Proc. Natl. Acad. Sci. USA.* 93: 2095–2099.

Nedkov, P., V. Spassov, and S. Tzokov. 1996. Relationship between accessibility and reactivity of Lys, Met and Tyr in subtilisins DY and Carlsberg. *Biol. Chem.* 377:653–659.

Nimigean, C.M., and K.L. Magleby. 1999. The beta subunit increases the Ca^{2+} sensitivity of large conductance Ca^{2+}-activated potassium channels by retaining the gating in the bursting states. *J. Gen. Physiol.* 113:425–440.

Nimigean, C.M., and K.M. Magleby. 2000. Functional coupling of the β1 subunit to the large conductance Ca^{2+}-activated K^+ channel in the absence of Ca^{2+}: increased Ca^{2+} sensitivity from a Ca^{2+}-independent mechanism. *J. Gen. Physiol.* 115:719–736.

Noceti, F., P. Baldelli, X.Y. Wei, N. Qin, L. Toro, L. Birnbaumer, and E. Stefani. 1996. Effective gating charges per channel in voltage-dependent K^+ and Ca^{2+} channels. *J. Gen. Physiol.* 108:143–155.

Olanow, C.W., and G.W. Arendash. 1994. Metals and free radicals in neurodegeneration. *Curr. Opin. Neurol.* 7:548–558.

Opie, L.H. 1989. Reperfusion injury and its pharmacologic modification. *Circulation.* 80:1049–1062.

Pallotta, B.S., A.L. Blatz, and K.L. Magleby. 1992. Recording from calcium-activated potassium channels. *Methods Enzymol.* 207:194–207.

Park, M.K., S.H. Lee, S.J. Lee, W.K. Ho, and Y.E. Earm. 1995. Different modulation of Ca-activated K channels by the intracellular redox potential in pulmonary and ear arterial smooth muscle cells of the rabbit. *Pflügers Arch.* 430:308–314.

Perozo, E., D.M. Cortes, and L.G. Cuello. 1999. Structural rearrangements underlying K^+-channel activation gating. *Science.* 285:73–78.

Pluger, S., J. Faulhaber, M. Furstenau, M. Lohn, R. Waldschutz, M. Gollasch, H. Haller, F.C. Luft, H. Ehmke, and O. Pongs. 2000. Mice with disrupted BK channel ss1 subunit gene feature abnormal Ca^{2+} Spark/STOC coupling and elevated blood pressure. *Circ. Res.* 87:E53–E60.

Quinonez, M., M. DiFranco, and F. Gonzalez. 1999. Involvement of methionine residues in the fast inactivation mechanism of the sodium current from toad skeletal muscle fibers. *J. Membr. Biol.* 169: 83–90.

Rahman, M.A., H. Nelson, H. Weissbach, and N. Brot. 1992. Cloning, sequencing, and expression of the *Escherichia coli* peptide methionine sulfoxide reductase gene. *J. Biol. Chem.* 267:15549–15551.

Ramanathan, K., T.H. Michael, G.J. Jiang, H. Hiel, and P.A. Fuchs. 1999. A molecular mechanism for electrical tuning of cochlear hair cells. *Science.* 283:215–217.

Rettig, J., S.H. Heinemann, F. Wunder, C. Lorra, D.N. Parcej, J.O. Dolly, and O. Pongs. 1994. Inactivation properties of voltage-gated K^+ channels altered by presence of β-subunit. *Nature.* 369: 289–294.

Rothberg, B.S., and K.L. Magleby. 1998. Kinetic structure of large-conductance Ca^{2+}-activated K^+ channels suggests that the gating includes transitions through intermediate or secondary states. A mechanism for flickers. *J. Gen. Physiol.* 111:751–780.

Rothberg, B.S., and K.L. Magleby. 1999. Gating kinetics of single large conductance Ca^{2+}-activated K^+ channels in high Ca^{2+} suggest a two-tiered allosteric gating mechanism. *J. Gen. Physiol.* 114: 93–124.

Rubanyi, G.M. 1988. Vascular effects of oxygen-derived free radicals. *Free Radic. Biol. Med.* 4:107–120.

Ruppersberg, J.P., M. Stocker, O. Pongs, S.H. Heinemann, R. Frank, and M. Koenen. 1991. Regulation of fast inactivation of cloned mammalian IK(A) channels by cysteine oxidation. *Nature.* 352:711–714.

Rusch, N.J., Y. Liu, and K.A. Pleyte. 1996. Mechanisms for regulation of arterial tone by Ca^{2+}-dependent K^+ channels in hypertension. *Clin. Exp. Pharmacol. Physiol.* 23:1077–1081.

Sanders, D.B., T. Kelley, and D. Larson. 2000. The role of nitric oxide synthase/nitric oxide in vascular smooth muscle control. *Perfusion.* 15:97–104.

Schlief, T., R. Schönherr, and S.H. Heinemann. 1996. Modification of C-type inactivating *Shaker* potassium channels by chloramine-T. *Pflügers Arch.* 431:483–493.

Schreiber, M., and L. Salkoff. 1997. A novel calcium-sensing domain in the BK channel. *Biophys. J.* 73:1355–1363.

Schreiber, M., A. Yuan, and L. Salkoff. 1999. Transplantable sites confer calcium sensitivity to BK channels. *Nat. Neurosci.* 2:416–421.

Shechter, Y., Y. Burstein, and A. Patchornik. 1975. Selective oxidation of methionine residues in proteins. *Biochemistry.* 14:4497–4503.

Shen, K.Z., A. Lagrutta, N.W. Davies, N.B. Standen, J.P. Adelman, and R.A. North. 1994. Tetraethylammonium block of Slowpoke calcium-activated potassium channels expressed in *Xenopus* oocytes: evidence for tetrameric channel formation. *Pflügers Arch.* 426:440–445.

Shriver, Z., Y. Hu, K. Pojasek, and R. Sasisekharan. 1998. Heparinase II from *Flavobacterium heparinum.* Role of cysteine in enzymatic activity as probed by chemical modification and site-directed mutagenesis. *J. Biol. Chem.* 273:22904–22912.

Silberberg, S.D., A. Lagrutta, J.P. Adelman, and K.L. Magleby. 1996. Wanderlust kinetics and variable Ca^{2+}-sensitivity of *Drosophila*, a large conductance Ca^{2+}-activated K^+ channel, expressed in oocytes. *Biophys. J.* 70:2640–2651.

Singer, J.J., and J.V. Walsh, Jr. 1987. Characterization of calcium-activated potassium channels in single smooth muscle cells using the patch-clamp technique. *Pflügers Arch.* 408:98–111.

Song, L., and K.L. Magleby. 1994. Testing for microscopic reversibility in the gating of maxi K^+ channels using two-dimensional dwell-time distributions. *Biophys. J.* 67:91–104.

Southam, E., and J. Garthwaite. 1996. Nitric oxide-cyclic GMP pathway in brain slices. *Methods Enzymol.* 269:129–133.

Stadtman, E.R., and B.S. Berlett. 1998. Reactive oxygen-mediated protein oxidation in aging and disease. *Drug Metab. Rev.* 30:225–243.

Stamler, J.S. 1994. Redox signaling: nitrosylation and related target interactions of nitric oxide. *Cell.* 78:931–936.

Stefani, E., M. Ottolia, F. Noceti, R. Olcese, M. Wallner, R. Latorre, and L. Toro. 1997. Voltage-controlled gating in a large conductance Ca^{2+}-sensitive K^+ channel (hslo). *Proc. Natl. Acad. Sci. USA.* 94:5427–5431.

Stephens, G.J., D.G. Owen, and B. Robertson. 1996. Cysteine-modifying reagents alter the gating of the rat cloned potassium channel Kv1.4. *Pflügers Arch.* 431:435–442.

Stief, T.W., J. Kurz, M.O. Doss, and J. Fareed. 2000. Singlet oxygen inactivates fibrinogen, factor V, factor VIII, factor X, and platelet aggregation of human blood. *Thromb. Res.* 97:473–480.

Suzuki, Y.J., H.J. Forman, and A. Sevanian. 1997. Oxidants as stimulators of signal transduction. *Free Radic. Biol. Med.* 22:269–285.

Talukder, G., and R.W. Aldrich. 2000. Complex voltage-dependent behavior of single unliganded calcium-sensitive potassium channels. *Biophys. J.* 78:761–772.

Tanaka, Y., P. Meera, M. Song, H.G. Knaus, and L. Toro. 1997. Molecular constituents of maxi KCa channels in human coronary smooth muscle: predominant alpha + beta subunit complexes. *J. Physiol.* 502:545–557.

Thuringer, D., and I. Findlay. 1997. Contrasting effects of intracellular redox couples on the regulation of maxi-K channels in isolated myocytes from rabbit pulmonary artery. *J. Physiol.* 500:583–592.

Toro, L., and E. Stefani. 1991. Calcium-activated K^+ channels: metabolic regulation. *J. Bioenerg. Biomembr.* 23:561–576.

Toro, L., M. Wallner, P. Meera, and Y. Tanaka. 1998. Maxi-K_{Ca}, a unique member of the voltage-gated K channel superfamily. *News Physiol. Sci.* 13:112–117.

Vaandrager, A.B., and H.R. de Jonge. 1996. Signalling by cGMP-dependent protein kinases. *Mol. Cell. Biochem.* 157:23–30.

Vergara, C., R. Latorre, N.V. Marrion, and J.P. Adelman. 1998. Calcium-activated potassium channels. *Curr. Opin. Neurobiol.* 8:321–329.

Vogt, W. 1995. Oxidation of methionyl residues in proteins: tools, targets and reversal. *Free Radic. Biol. Med.* 18:93–105.

Wallner, M., P. Meera, M. Ottolia, G.J. Kaczorowski, R. Latorre, M.L. Garcia, E. Stefani, and L. Toro. 1995. Characterization of and modulation by a beta-subunit of a human maxi K_{Ca} channel cloned from myometrium. *Receptors Channels.* 3:185–199.

Wallner, M., P. Meera, and L. Toro. 1996. Determinant for beta-subunit regulation in high-conductance voltage-activated and Ca^{2+}-sensitive K^+ channels: an additional transmembrane region at the N terminus. *Proc. Natl. Acad. Sci. USA.* 93:14922–14927.

Wang, G.K., M.S. Brodwick, and D.C. Eaton. 1985. Removal of sodium channel inactivation in squid axon by the oxidant chloramine-T. *J. Gen. Physiol.* 86:289–302.

Wang, Z.W., M. Nara, Y.X. Wang, and M.I. Kotlikoff. 1997. Redox regulation of large conductance Ca^{2+}-activated K^+ channels in smooth muscle cells. *J. Gen. Physiol.* 110:35–44.

Wanner, S.G., R.O. Koch, A. Koschak, M. Trieb, M.L. Garcia, G.J. Kaczorowski, and H.G. Knaus. 1999. High-conductance calcium-activated potassium channels in rat brain: pharmacology, distribution, and subunit composition. *Biochemistry.* 38:5392–5400.

Wei, A., C. Solaro, C. Lingle, and L. Salkoff. 1994. Calcium sensitivity of BK-type K_{Ca} channels determined by a separate domain. *Neuron.* 13:671–681.

Wood, L.S., and G. Vogeli. 1997. Mutations and deletions within the S8-S9 interdomain region abolish complementation of N- and C-terminal domains of Ca^{2+}-activated K^+ (BK) channels. *Biochem. Biophys. Res. Commun.* 240:623–628.

Yellen, G. 1984. Relief of Na^+ block of Ca^{2+}-activated K^+ channels by external cations. *J. Gen. Physiol.* 84:187–199.

Yellen, G. 1998. The moving parts of voltage-gated ion channels. *Quart Rev. Biophys.* 31:239–296.

Yellen, G., M.E. Jurman, T. Abramson, and R. MacKinnon. 1991. Mutations affecting internal TEA blockade identify the probable pore-forming region of a K^+ channel. *Science.* 251:939–942.

Zanzinger, J. 1999. Role of nitric oxide in the neural control of cardiovascular function. *Cardiovasc. Res.* 43:639–649.